DPST-78-128-1/2

SAVANNAH RIVER LABORATORY MONTHLY REPORT

^{238}Pu FUEL FORM PROCESSES JANUARY/FEBRUARY 1978

Approved by:

R. T. Huntoon, Research Manager
Nuclear Materials Division

E. I. DU PONT DE NEMOURS AND COMPANY
SAVANNAH RIVER LABORATORY
AIKEN, SOUTH CAROLINA 29801

PREPARED FOR THE U.S. DEPARTMENT OF ENERGY UNDER CONTRACT AT(07-2)-1

DISCLAIMER

CONTENTS

FOREWORD

This report is one of a series to summarize progress in the Savannah River ^{238}Pu Fuel Form Program. This program is supported primarily by the DOE Division of Advanced Systems and Materials Production (DASMP), and also by the Division of Military Applications (DMA).

Goals of the Savannah River Laboratory (SRL) program are: to provide technical support for the transfer of DASMP and DMA ^{238}Pu fuel form fabrication operations from Mound Laboratory to new facilities at the Savannah River Plant (SRP), to provide the technical basis for ^{238}Pu scrap recovery at SRP, and to assist in sustaining plant operations. This part of the program includes:

Demonstration of processes and techniques, developed by the Los Alamos Scientific Laboratory (LASL) and Monsanto Research Corporation (MRC), for production at SRP. Information from the demonstration will provide the technical data for technical standards and operating procedures.

Technical Support to assist plant startup and to ensure continuation of safe and efficient production of high-quality heat-source fuel.

Technical Assistance after startup to accommodate changes in product and product specifications, to assist user agencies in improving product performance, to assist SRP in making process improvements that increase efficiency and product reliability, and to adapt plant facilities for new products.

MULTI-HUNDRED WATT PROCESS DEMONSTRATION

FABRICATION OF PREPRODUCTION MHW SPHERES

A tenth MHW sphere was hot-pressed in the PuFF Facility in January in an attempt to duplicate process conditions used to fabricate Sphere 9, the best of the three spheres shipped to MRC.[1] Sphere 10, however, developed observable cracks on exposure to oxygen at self-heat temperatures following hot pressing, and fractured during the post-hot-pressing heat treatment. Failure of this sphere further indicates that suitable centerline conditions for one or more critical process steps have not been established, or that processing variability has been excessive. The former is believed to be the primary reason for sphere failures as described in the next section.

Sphere 10 was fabricated using centerline conditions similar to those used in pressing Spheres 7 through 9. Table 1 compares recorded processing data for the three spheres shipped to MRC (Spheres 2, 8, and 9) and for Sphere 10.

Sphere 10 was crack-free on removal from the die. The belly-band of the sphere was well formed, with no visible effects of punch erosion. Equatorial and polar sphere diameters of the as-pressed sphere were 1.437 in. and 1.440 in., respectively, considerably below the specified diameter of 1.465 ±0.015 in. for a heat-treated sphere. Density calculated from as-pressed dimensions was 89% TD, which is greater than those of previous as-pressed spheres.

After Sphere 10 was gaged, it remained overnight (about 14 hr) in a thoria dish in the heat-treatment furnace at self-heat temperatures (estimated 500 to 700°C) under argon cell atmosphere. The sphere was then exposed to flowing $^{16}O_2$ for one hour in the furnace prior to re-examination and weighing. Surface inspection revealed a few large cracks had formed in the sphere, as illustrated in Figure 1. A second one-hour exposure at self-heat temperatures to flowing $^{16}O_2$ in the furnace produced possibly one additional crack, also indicated in Figure 1. Final heat-treatment at high temperature (nominally 1410°C, although possibly at much higher temperature, as indicated in subsequent section) in $^{16}O_2$ atmosphere widened existing cracks and formed additional large cracks (Figure 2). The sphere fractured (Figure 3) before dimensional measurements could be made. The weight gain after exposures, given in Table 2, indicate the extent of oxidation that occurred in each of the post-hot-pressing operations.

TABLE 1

Process Conditions for MHW Spheres

Process Step	*Goal*	*Sphere* 2	8	9	10
Oxygen Exchange;					
Time, hr	5	5	5	4	5
Temp, °C	800	785	800	800	840
Outgas					
Time, hr	1	1	∿1 ∿1	∿1 ∿1.5	∿1
Temp, °C	100	940	990 1000	1000 1000	990
$^{16}O_2$ Flow, cc/min	40	40	40 32	32 42	40
Ball Mill					
Time, hr	12	12	12	12	12
Cold Press					
Pressure, psi	58,000	56,000	57,800	58,200	58,200
Particle Size, μm	<125	<125	<125	<125	<125
Sintering					
Time, hr	6	1½-2 3	6	5.5-6	6
Temp, °C	1175	1130-1155[a] 1175-1190[a]	1175[a]	1170[a]	1150[a]
Hot Press					
Time, min	30	30	30	30	30
Temp, °C	1490	1495	>1520[b]	>1490[b]	1490[c]
Force, lb	5050(3000 psi)	5070	5060	5050	5060
Heat Treatment					
Time, hr	12	10.5	11.5	11.5	11-12
Temp, °C	1440	1440-1450	1450	1440	1410
$^{16}O_2$ Flow, cc/min	19	40	19	19	19
Ar Flow, cc/min	900	0	650-680	650	900

a. Indicated temperatures from temperature records. Cold junction correction is not necessary.

b. Inside surface of view window was dirty. This is estimated to have been worth another 20-50°C added to temperature shown.

c. Inside surface of view window very dirty — estimated to be worth 50-100°C added to temperature shown.

Top Polar View

(Hemisphere formed in top punch)

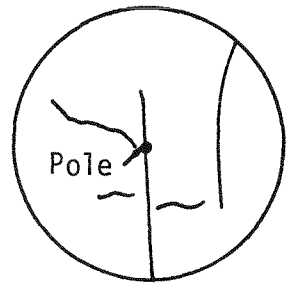

Equatorial View

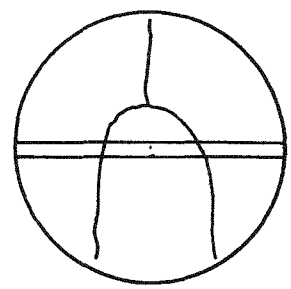

Bottom Polar View

(Hemisphere formed in bottom punch)

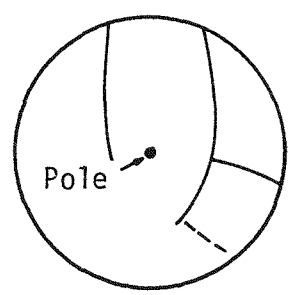

Additional crack possibly formed during 2nd hour exposure to flowing $^{16}O_2$

FIGURE 1. Appearance of Surface Cracks in As-Pressed Sphere 10 Following Low Temperature Oxidation. The sphere was exposed to $^{16}O_2$ for one and two hours at self-heat temperatures after standing overnight in cell argon atmospheres.

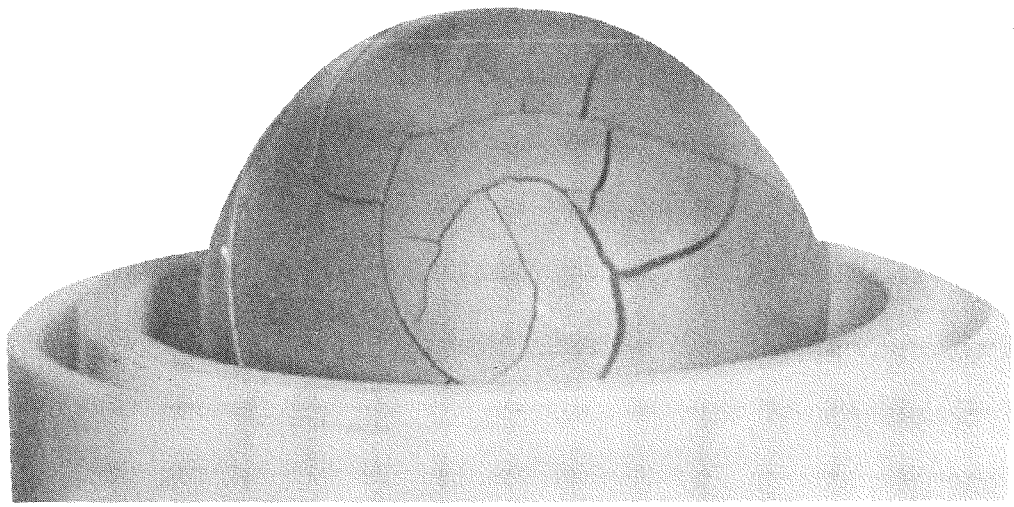

A. Bottom Hemisphere

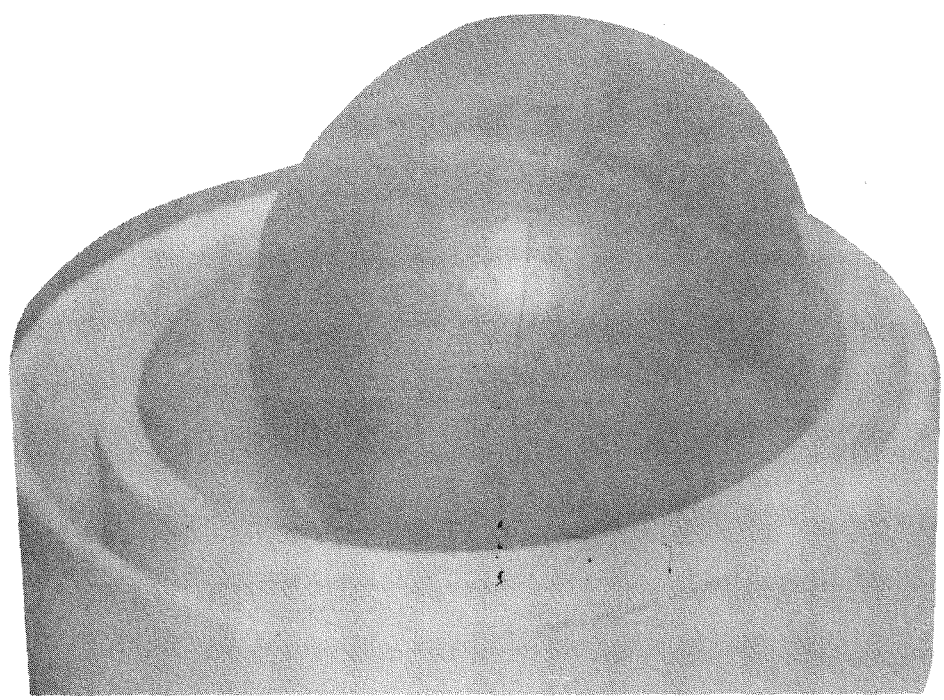

B. Top Hemisphere

FIGURE 2. Surfaces of Sphere 10 After Final Heat Treatment at High Temperatures (1410°C) in $^{16}O_2$ Atmosphere. The surfaces shown represent the condition of the sphere soon after removal from the furnace.

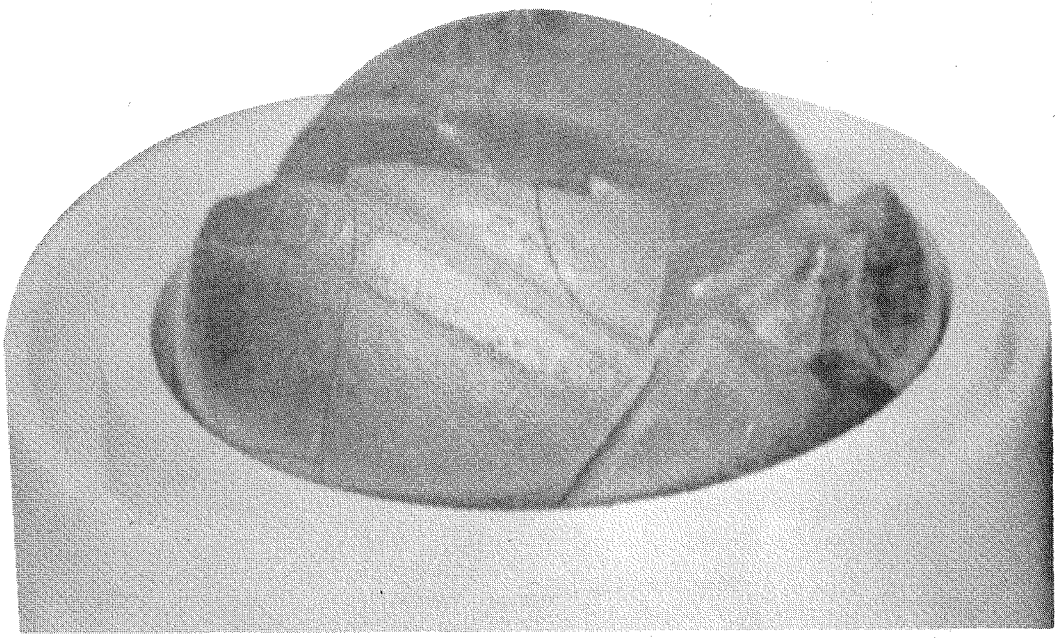

FIGURE 3. Appearance of Sphere 10 After Fracture. Top hemisphere is in foreground and bottom hemisphere is in background.

TABLE 2

Weight Changes of Sphere 10 During Fabrication[a]

Weight of Powder Charged to Die	252.71
Weight of As-Pressed Sphere	250.84
Weight Loss During Hot Pressing	1.87
Weight Gain on Standing Overnight in Cell Atmosphere Followed by 1-hr Exposure of Flowing $^{16}O_2$	0.61
Weight Gain During Additional 1-hr Exposure to Flowing $^{16}O_2$	0.20
Weight Gain During Final Heat Treatment	1.10
Total Weight Gain During Reoxidation	1.91

a. All weights in grams.

Examination of fractured sphere segments showed a primary fracture along the equatorial plane through the belly-band, and several secondary transpolar fractures in the resulting hemispheres (Figure 4). The fractured segments showed cracking patterns of two types: (1) surface cracks extending radially a short distance into the sphere interior, and (2) a nugget of severely cracked interior material near the center of the sphere. The radial surface cracks, which decreased in thickness with depth into the sphere, were apparently formed during reoxidation of the sphere prior to and during the initial stages of final heat treatment. The severe cracking in the core of Sphere 10 is very similar to cracking observed in core regions of high-density, hot-pressed $^{239}PuO_2$ pellets that were heat-treated under conditions intended to distinguish between reoxidation cracking and other crack-generating mechanisms.[2] In the $^{239}PuO_2$ work, core cracking was attributed to reoxidation effects during heat treatment; i.e., volume reduction on phase change and CO_2 pressurization at grain boundaries. Anisotropic shrinkage from sintering during final heat treatment and thermal stresses probably also contributed to the cracks observed in Sphere 10.

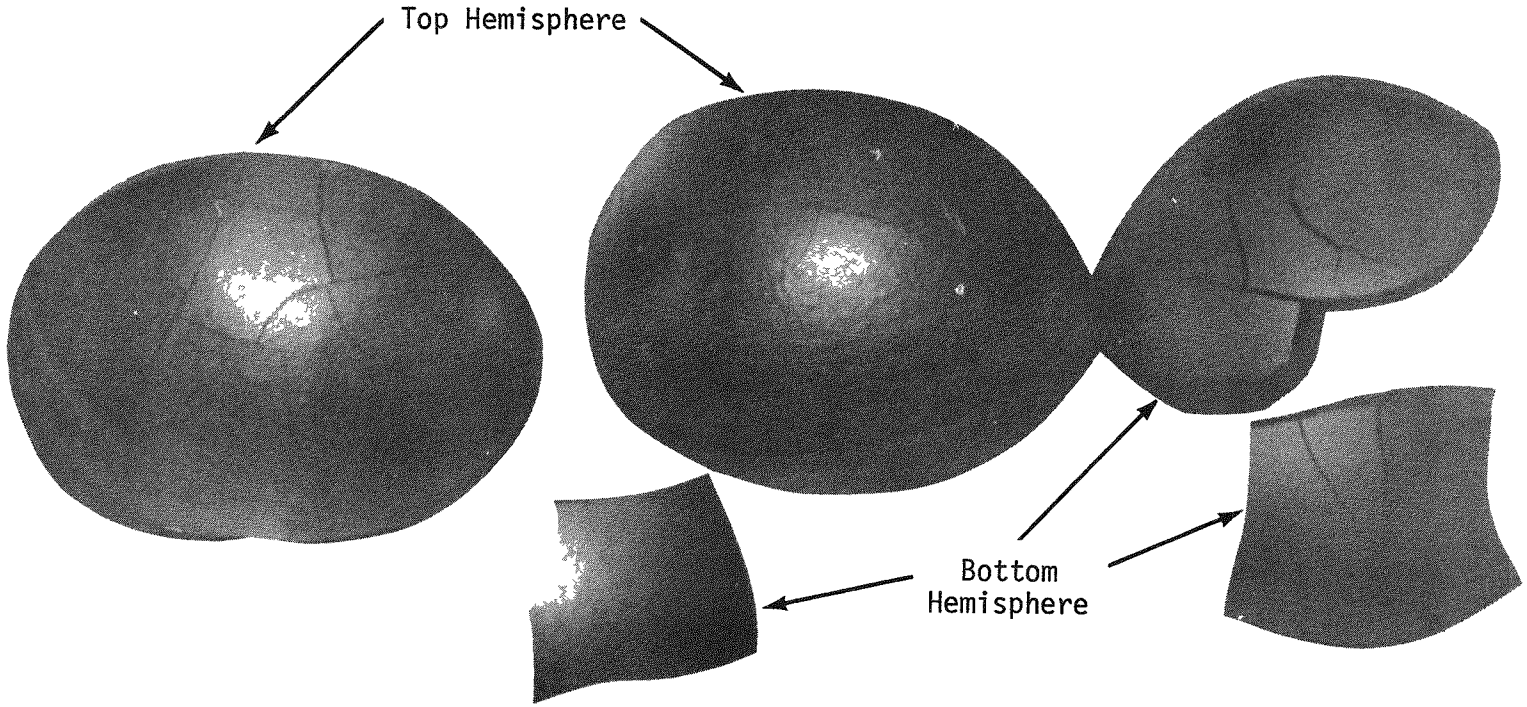

a. View of Spherical Surfaces

FIGURE 4. Segments of Fractured Sphere 10

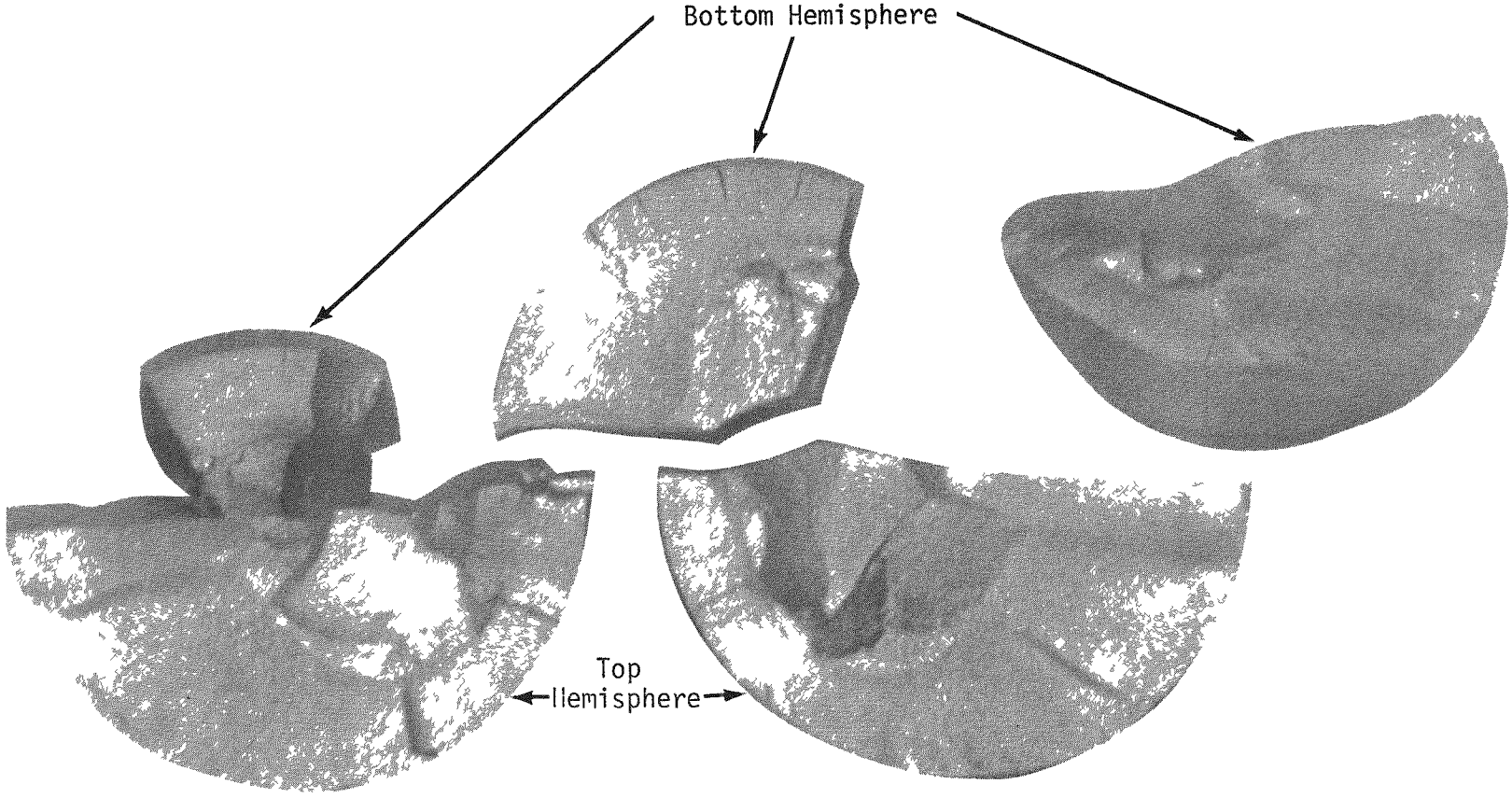

b. View of Fracture Surfaces Parallel to Equatorial Plane

FIGURE 4 (continued)

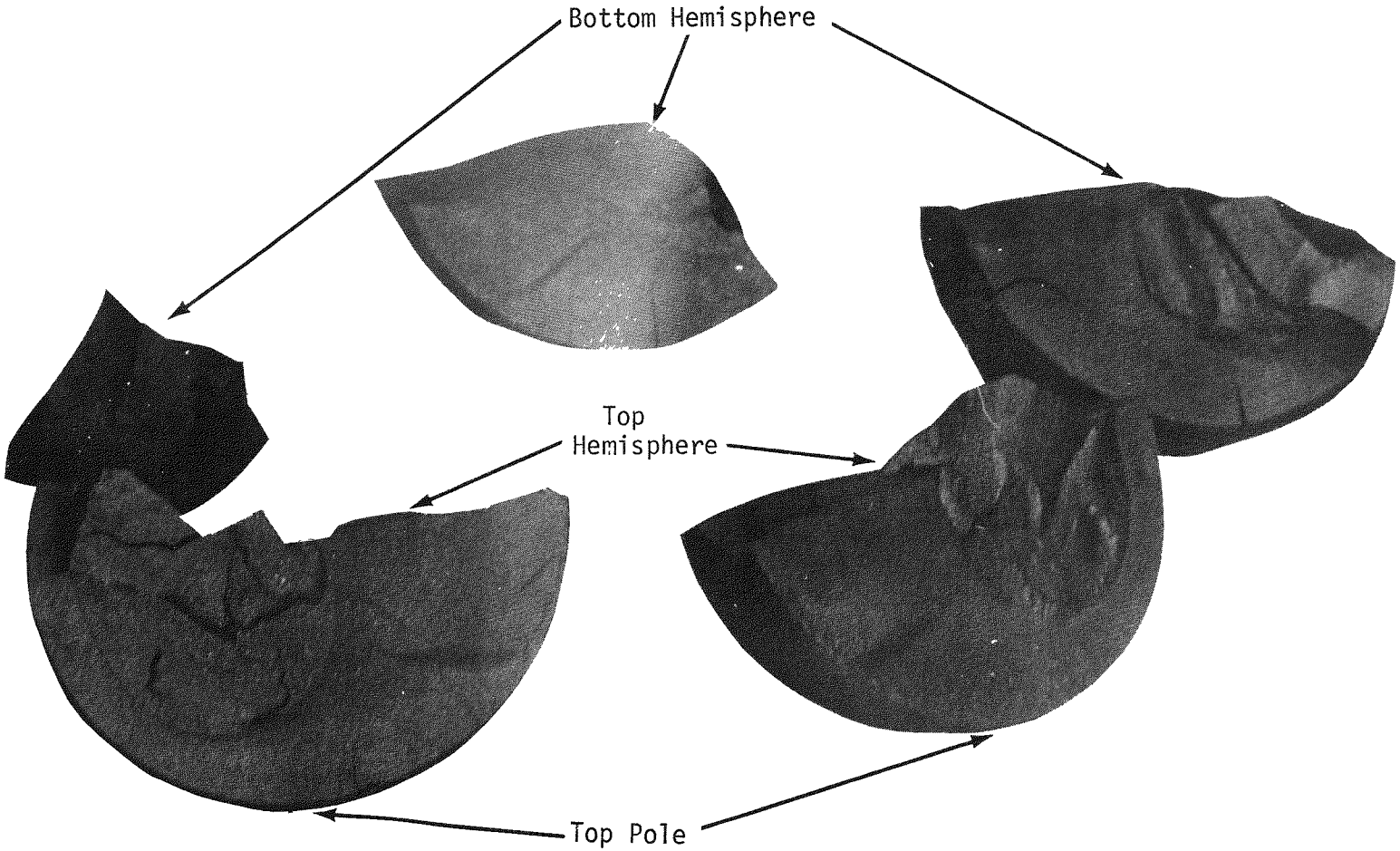

c. View of Fracture Surfaces Perpendicular to Equatorial Plane

FIGURE 4. (Continued)

EXCESSIVE DENSIFICATION AND FRACTURE OF PREPRODUCTION SPHERES

The previous monthly report[1] described probable causes of fracture of MHW spheres made during the preproduction program in the PuFF Facility: excessive and nonuniform densities produced in hot-pressed fuel, reoxidation effects during self-heating and final heat treatment, anisotropic shrinkage from sintering during heat treatment, and thermal stresses. Accumulating evidence, primarily metallographic analyses, indicates the principal factor leading to cracked, undersized, and too-dense MHW spheres in the PuFF Facility is excessive pressure and rate of application during hot pressing. Another factor, shard quality, appears to be of secondary importance within the variability of PuFF experience.

High, rapidly applied pressure causes the shards to break and repack more compactly. As a result, the as-pressed spheres have major regions of excessive density and undesirable microstructure (no stable, coarse intershard porosity) which are susceptible to cracking during subsequent handling, reoxidation, and heat treatment. Major portions of the spheres are significantly above 85% TD, a density above which cracking occurs on reoxidation apparently because of volume change and/or CO_2 gas pressurization.[2] The propensity to fracture on the equatorial plane is also aggravated by the high pressing pressures.[1] Higher effective pressures in the PuFF hot press for the same applied load as was used by LASL are believed to result from differences between the SRP and LASL die designs and pressing modes (double action versus single action).

Large grain sizes and patterns of microcracks, also revealed by metallographic analysis of spheres, indicate post-hot-pressing heat-treatment temperatures have been too high.

EVIDENCE FOR EXCESSIVE HOT-PRESSING PRESSURE

Differences in Die Design and Pressing Mode

The persistent production of unacceptable spheres, in spite of many equipment and parameter adjustments throughout the process, indicates that a major factor in process or equipment is at fault. The one departure from the LASL process that might have a major role in determining sphere properties is the design of the hot-press die assembly and the mode of utilizing the hot press. LASL developed the process using a two-piece die assembly pressed in single action, i.e., only one punch moving. The Savannah River process has a three-piece die assembly with both rams moving during compaction.

Die closure has been observed in the PuFF pressings generally in about half the time or less than in pressings by LASL, i.e., 1 to 5 min. versus 10 to 12 min. This observation, combined with the observation in tests made in the Alpha Materials Facility (AMF) that closure rate varies with applied load, suggests higher effective pressures for the PuFF die configuration and pressing mode. Application of load on both punches simultaneously rather than on one punch evidently increases the effective pressure on the powder and alters the distribution of pressing forces to accomplish more densification at the same applied load.

The relatively poor and variable flow characteristics of the shards in the die probably amplify the differences between single- and double-action compaction. This effect is supported by observations made in pellet pressings in the AMF. Shards with large differences in pour and tapped densities produced observable differences in density distribution in small pellets pressed in the single- versus double-action modes.

The independent translation and expansion of the die body relative to the punches in the three-piece PuFF die may aggravate the stress concentration at the belly-band, a predominant plane of fracture observed in PuFF spheres (previous section this report and November-December 1977 report[1]). In contrast, LASL hot-presses spheres into a "cup," i.e., a one-piece lower punch and die body. The compression ratio at the knife edges of hemispherical punches is at least ten times greater than at the poles, so that discontinuities at the belly-band may be enlarged and powder flow in the belly-band region may be significantly altered in spherical die assemblies.

Density As Pressed

The densities of 8 of the 10 spheres for which measurements were made after hot pressing and before post-hot press heat-treatment were too high, 82 to 89% TD,[1] versus the desired 81%. High densities can result from excessive hot-pressing pressure and temperature and from high shard sinterability. Higher pressure would be expected to produce higher densities by breaking up shards to promote better compaction and more shrinkage during hot pressing. This increased densification should be most prevalent at the equator where compressive loads are highest. The effects were observable in the metallographic analyses described below.

Differences in Cold-Press Tests of Spherical Dies

Large differences were reported[1] between single- and double-action compaction using three-piece PuFF die assemblies to cold press simulant powders. These tests showed that (1) there are

large differences in the flow and density characteristics within spheres compacted by single- and double-action at the same applied load; (2) powders densified most in the belly-band region in both cases; (3) powders compacted into spheres tend to fracture in the equatorial plane at the corner of the belly-band (juncture between the knife edges of the punches and the die wall); and (4) double-action compaction produces higher stress concentration in the belly-band region than does single-action compaction for the same applied load. Cracking and fracture observed in PuFF spheres always included part of the equatorial plane at the corner of the belly-band.

Microstructures of PuFF Spheres

The strongest evidence of high or rapidly applied hot-pressing pressure is the observed microstructures of three preproduction spheres compared to those of pellets made in parametric studies in the AMF and at LASL. Detailed descriptions and interpretations of the microstructures of the three spheres (Spheres 1, 4, and 5) are given later in this report. General features of the sphere microstructures are summarized below and compared to catalogued data from AMF parametric studies discussed in the next section.

- The PuFF microstructures are not typical of LASL MHW spheres. The shards were degraded during hot pressing so as to eliminate most of the coarse, stable, intershard porosity and destroy the identity of individual shards (Figure 5). The absence of stable, intershard porosity explains the observed excessive shrinkage that generally occurred on sintering.

- All seven pieces examined of the three spheres contained extensive networks of internal cracks and had metallographic densities from 88 to 95% TD, well into the density range, >85% TD, where previous work[2] showed fracture occurs on subsequent reoxidation.

- Equatorial pieces were more dense than polar or core pieces and showed predominant fracture emanating from the edge of the belly-band. This fracture pattern indicates excess stress concentration at the equator.

- Pieces from as-pressed Sphere 4, which had oxidized at ambient temperature, were considerably less fractured in spite of their high density. The few microcracks observed consisted of grain-boundary separations and the same microcracks obtained in low-temperature oxidation tests of dense $^{239}PuO_2$ pellets. These observations suggest that incipient cracking in high-density regions is caused predominantly by oxidation after hot pressing.

- Cracks were thin, sharp, and "fresh" in fuel that was oxidized at ambient temperatures and not heat treated. After heat treatment the fracture surfaces tended to become rounded and either widened or "healed." These observations indicate the cracks were formed after hot pressing or early in the post-hot-press heat treatment.

- A kernel of excessive cracking exists in the interior of the spheres. This region was especially broken up relative to the shell with fracture patterns reminiscent of CO_2 gas fracture observed at high density and temperature (1500°C) in $^{239}PuO_2$ pellets (Figure 3 of the September 1977 Report[2]).

- Grain sizes were much too large for the density measured and heat-treatment temperature planned (1440°C). This observation indicates the post-hot-press heat-treatment temperatures are too high by about 70°C.

Laboratory Parametric Tests

Several process variables are capable of causing high density in as-pressed fuel and thereby the subsequent cracking. However, pellet studies in the AMF have shown excessive hot press pressure to be the most likely cause.

Figure 5 shows the great difference between the sphere microstructure typified by Sphere 5 and the desired MHW microstructure obtained from a pellet made in the AMF. Parameters most likely to produce undesirable sphere microstructure are density and strength of the shards, hot-press pressure, hot-press temperature, and post-hot-press heat-treatment temperature. These parameters were intentionally varied in a series of earlier fabrication tests in the AMF to determine their effects on MHW pellets. Results of these tests are summarized below.

Increasing hot-pressing pressure in pellet tests caused exactly the microstructural effect that was observed in Spheres 1, 4, and 5. $^{238}PuO_2$ pellets were pressed in the AMF using the same conditions as used in the PuFF Facility except the pressure on the single-action press was 5000 psi versus 3000 psi applied in the PuFF Facility press. The pellet pressed at 5000 psi had a microstructure similar to that of Spheres 1, 4, and 5; the pellet pressed at 3000 psi had a structure characterized by large, well-distributed pores and clearly discernible, unbroken shards (Figure 6). Application of excess pressure is the easiest way to break down the shards, eliminate coarse intershard porosity, and hence promote excessive sintering and shrinkage during hot pressing.

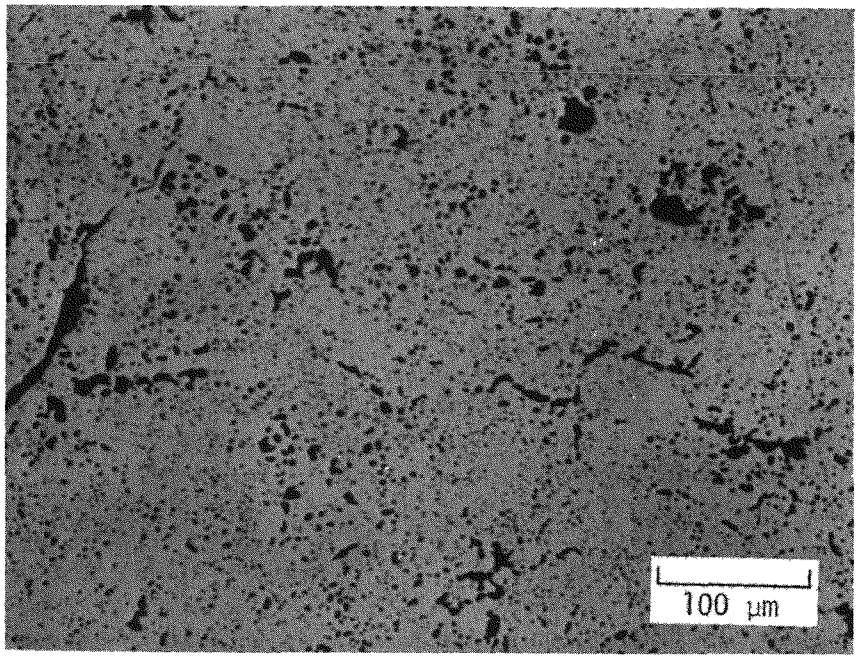

PuFF Sphere 5

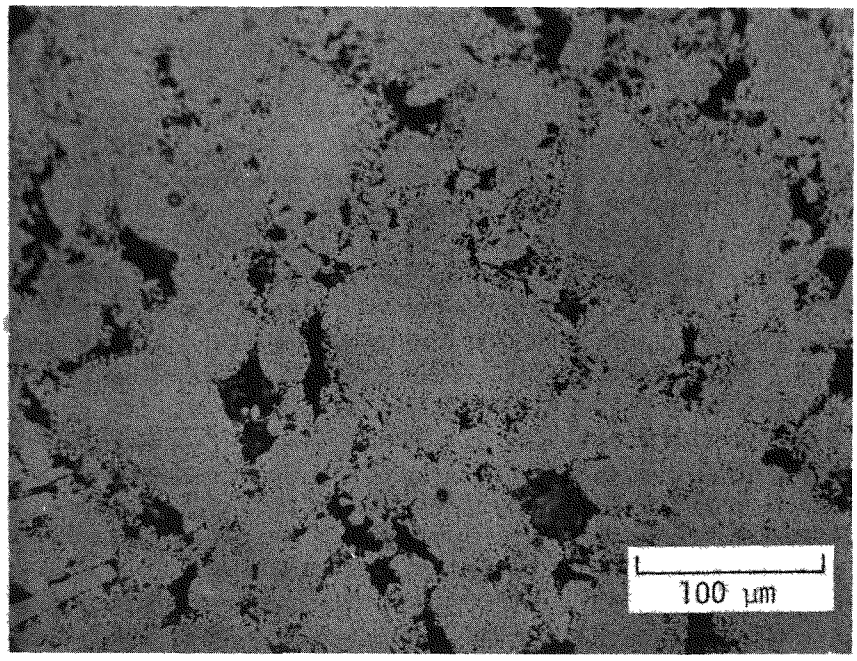

Desired Microstructure (Pellet)

FIGURE 5. Comparison of Microstructures Obtained in PuFF Sphere with the Desired Microstructure

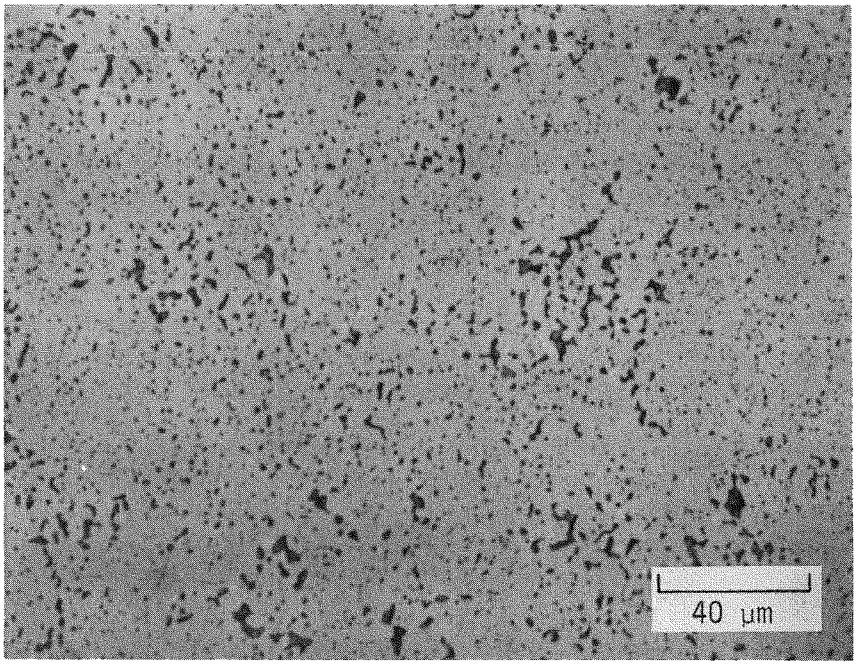

5000 psi

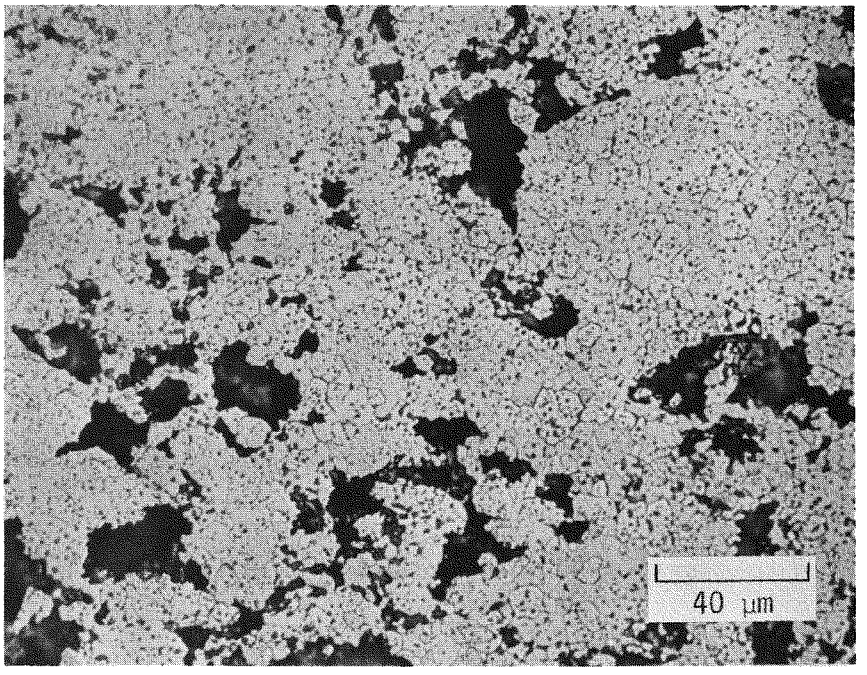

3000 psi

FIGURE 6. Effect of Hot-Press Pressure on Microstructure of Pellet

Lower shard presintering temperatures tend to produce a similar microstructure, but coarse porosity still remains. Figure 7 shows the microstructures of pellets pressed at 3000 psi in single-action dies using shards presintered at 1050°C and 1150°C. Distinct shards with surrounding coarse pores are predominant in the fairly typical MHW microstructure when denser shards presintered at 1150°C were used (Figure 7b). When less-dense, and hence weaker shards (produced at the lower 1050°C presintering temperature) were hot pressed, a more dense structure is obtained (Figure 7a). However, even though the individual shards are not distinct, coarse pores are still present, in contrast to the absence of such coarse porosity in the PuFF Spheres.

The combination of a low presintering temperature with high pressure (Figure 1 of the May 1977 report[3]) eliminates the coarse intershard porosity and produces dense microstructures typical of those in PuFF spheres. For denser shards obtained by presintering shards above 1150°C, however, the identity of the shards and coarse intershard porosity are still maintained even at higher hot-press pressure. The combination of dense shards and high hot-pressing pressure is, in fact, somewhat typical of the processing of MHW fuel at Mound Laboratory (MRC). Sphere 3, which was highly resistant to fracture in the as-pressed condition,[1] was pressed from "oversintered" shards (heated up to 12 hr at temperatures above the normal 1175°C), and represented a partially successful attempt at achieving a fracture-stable sphere by hardening the shards. Hardening the shards too much, however, will result in a heterogeneous microstructure rather than the desired, more-homogeneous microstructure found in spheres made at LASL.

If weak shards are being produced in the PuFF Facility, they are probably not caused by too low a shard presintering temperature. Temperatures 100°C or more below the intended 1175°C temperature are very unlikely considering the calibration efforts on the presintering furnace.

Even though grain size of the examined spheres (see discussion below on sphere microstructures) indicates the post-hot-press heat-treatment temperature was too high, results of past parametric tests in the AMF indicate that excessive heat-treatment temperatures cannot produce the microstructures observed in the PuFF spheres. Figure 8 shows the effect of heat-treating as-pressed pellets at temperatures up to 1600°C using otherwise centerline process conditions. The coarse intershard pores in the desired microstructure cannot be sintered away. The shards must be crushed by pressure during hot pressing.

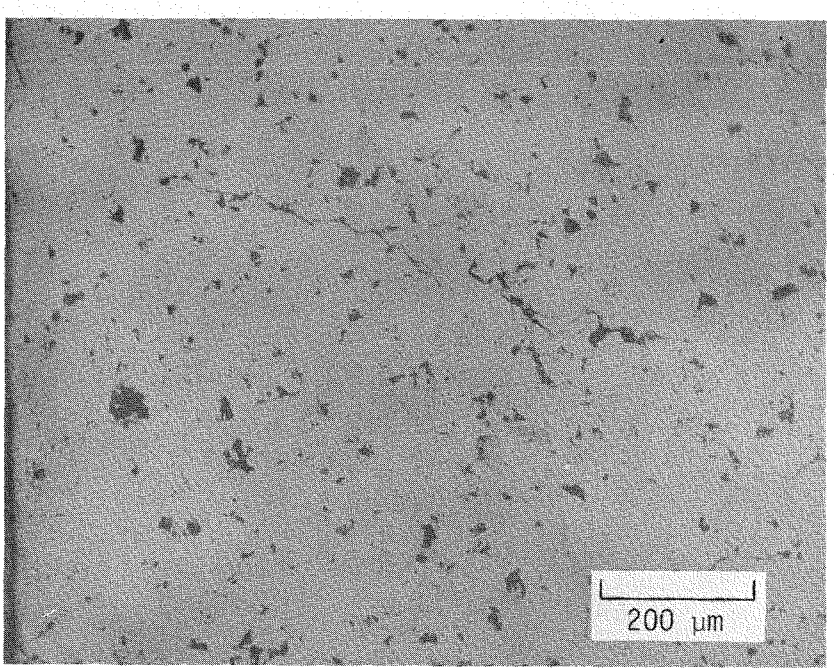

a. 1050°C, 3000 psi

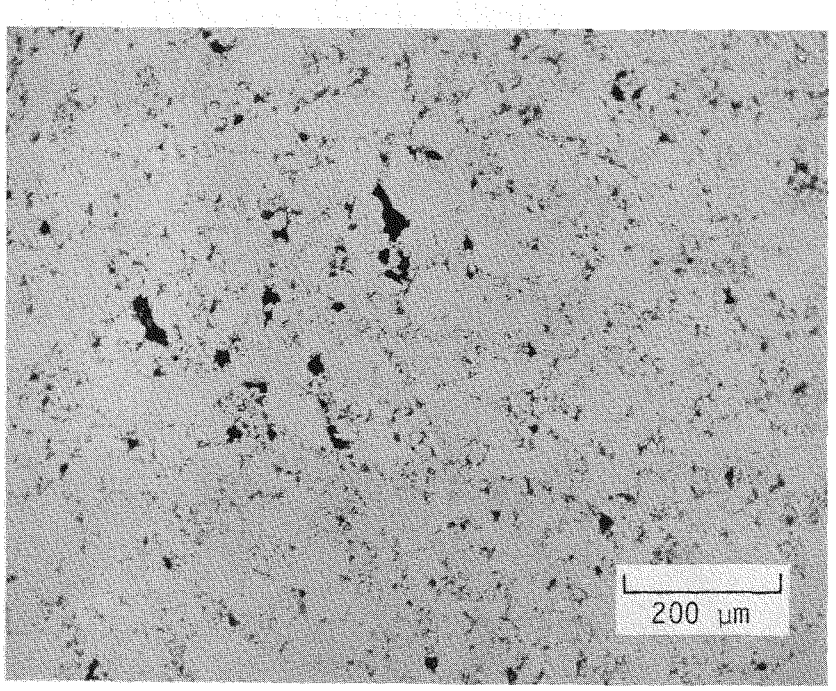

b. 1150°C, 3000 psi

FIGURE 7. Effect of Shard Presintering Temperature on Microstructure of Pellet.

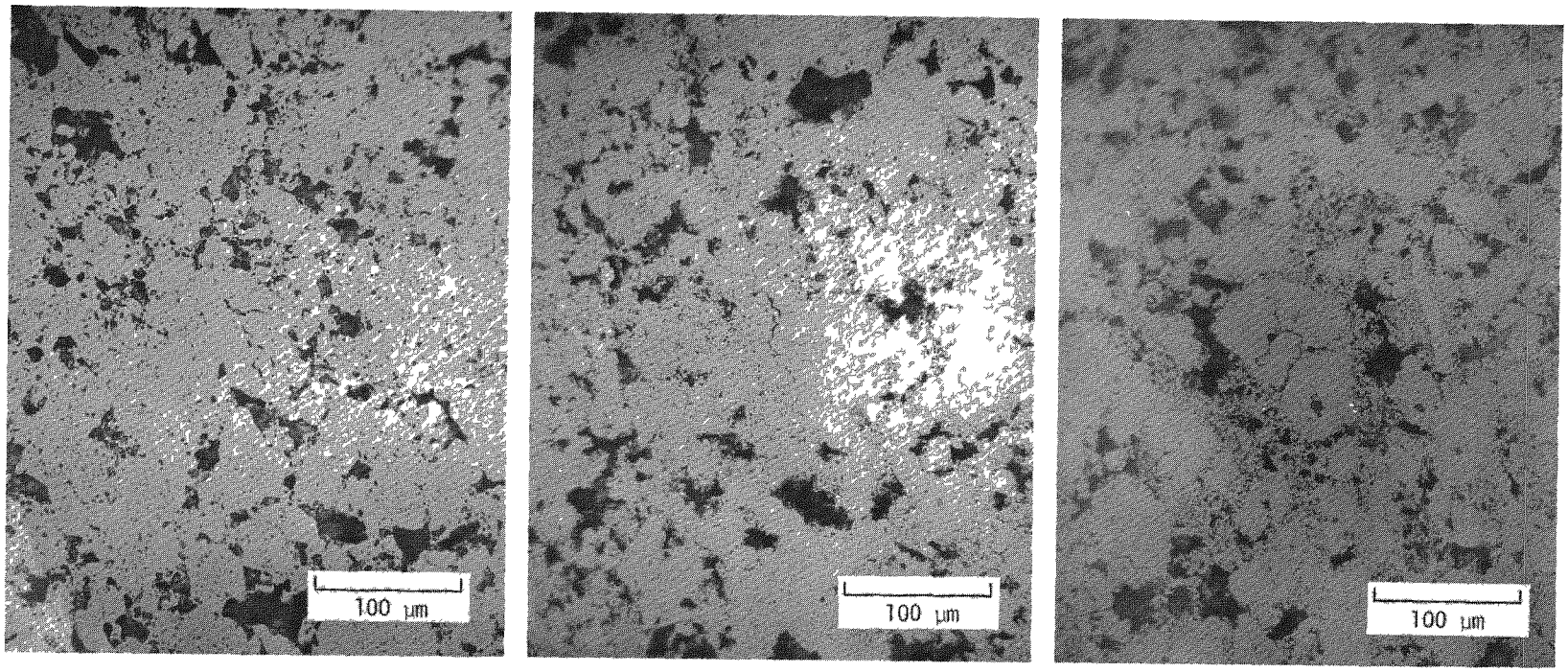

As-Pressed 1440°C 1600°C

FIGURE 8. Effect of Post-Hot-Press Heat Treatment on Microstructure

The effects of varying cold-press pressure, hot-press temperature or shard size on MHW microstructures were evaluated by LASL.[4] At normal hot-pressing pressure, shard identity and coarse intershard porosity are maintained when any of these three parameters are changed.

High Density Although Variable Shard Properties

The problem of high-density spheres containing crushed shards and undercut belly-bands has persisted in spite of some fairly wide variations in shard preparation, including under- and overmilled feed, low cold-press pressure, shards over twice nominal size, shards containing stainless steel, and shards presintered at both high and low temperatures. Despite these variations, the spheres were generally too dense.

Next to excessive hot-pressing pressure, the strength and sinterability of the shards are the most probable causes of the PuFF problems. However, because these variations in shard properties cannot be correlated with sphere properties, a more important factor is suspected, viz. hot-press pressure. This is not to say shard variability is not an important factor; it is just second order to pressing pressure.

The effects of feed powders and sharding conditions on shard strength and quality and the effects of shard quality on hot-pressed fuel are being investigated in a statistically designed parametric test in the PuFF Facility, as described in a subsequent section.

PROCESS OPTIONS FOR PuFF

The SRP mode of hot pressing by double action is a significant departure from the single-action compaction used at LASL. When the PuFF process was planned, both LASL and SRL expected that double action would produce even more uniform and homogenous spheres than could be obtained from single action and would be more effective for cylindrical GPHS fuel being developed at LASL. This improvement is still expected to be achieved.

The 5050-lb load (3000 psi pressure) recommended by LASL and presently used for hot pressing in PuFF is not consistent with the apparent greater effectiveness of double-action compaction. Although the parameters are the same, the microstructures are unacceptably different. To achieve a similar response in fuel structures requires either changing to the LASL single-action pressing mode, or, alternatively, reducing applied pressing pressure and the die closure rate to accommodate the differences in die design and press operation.

Another option is to increase the strength and decrease the sinterability of the shards (higher presintering temperature than 1175°C). However, changing shard characteristics in this way may require even higher hot-press pressure to produce the desired density. Higher pressure compaction of excessive presintered shards would produce spheres more like the MRC product with less homogeneity of microstructure.

Full-scale testing is required regardless of which option is chosen to find the parameters that will produce a suitable product. Pressing at lower pressure, rather than changing to the LASL pressing mode or increasing shard strength, is easier to accomplish and should produce the desired results. The distribution of microstructure in SRP spheres may be somewhat different than in LASL spheres, but it is not expected to differ enough to cause additional product evaluation beyond the certification presently planned. Since cracks have been observed in acceptable spheres made at both LASL and MRC, surface cracking may still occur in PuFF spheres even if lowering hot-press pressure produces integral and dimensionally stable spheres. Residual compaction stresses, stresses introduced on oxidation, and thermal gradients and transients may be expected to act synergistically to cause some cracking, but the product should be acceptable if it is within dimensional limits and not severely fractured.

Sphere pressing tests in the PuFF Facility to determine the effects of hot-press pressure reduction have been planned. Sphere 11 will be pressed at the lowest pressure and rate of application required to achieve die closure. Subsequent spheres will be pressed using different pressing ramps to bracket the acceptable pressing range for the PuFF press.

EVALUATION OF MICROSTRUCTURES OF PuFF SPHERES

The hypothesized mechanisms of cracking in $^{238}PuO_2$ fuel (reoxidation effects, compaction stresses, anisotropic shrinkage from differential sintering, and thermal stresses) have been discussed in past monthly reports. These mechanisms probably act synergistically to cause the cracking and fracture observed in MHW spheres produced in the PuFF Facility. As described below and summarized on pp. 18 and 19, the crack patterns and other microstructural characteristics observed in fragments from Spheres 1, 4, and 5 are very similar to those generated in test pellets fabricated under controlled laboratory conditions in the AMF to distinguish between reoxidation effects and other crack-generating mechanisms.[2] These comparisons suggest that the mechanisms most responsible for cracking of the first ten preproduction spheres may be those associated with reoxidation of the reduced, as-pressed fuel; i.e., the volume change occurring on phase change during oxidation and possible CO_2 gas pressurization at high temperature.

Sphere 1 (Heat Treated)

Figure 9 shows the as-polished cross section of three pieces of Sphere 1 that were chosen from among the several pieces present after post-hot-press heat-treatment. All three pieces exhibit networks of macro- and microcracks that are typical of those produced on oxidation of high-density PuO_{2-x} pellets.[2] The principal microcracks in the surface pieces are radial with a spacing averaging about 750 to 1000 μm. Cracks perpendicular to the surfaces of pellets having the same spacing were observed on reoxidizing dense pellets of $^{239}PuO_2$ between 600 and 1100°C in work yet to be reported.

Of the three spheres examined, the fragments from Sphere 1 were cracked most severely. These fragments were also the most dense. This observation is consistent with the observed increase in cracking severity with density that occurred on oxidizing reduced $^{239}PuO_2$ in earlier cracking studies.[2,5] Of the three pieces shown in Figure 9, the equatorial piece had the highest metallographic density, 95% of theoretical (TD), exclusive of macrocracks. This density is considerably in excess of the desired 82.5% TD and the 85% TD above which fracture on oxidation has been observed to consistently occur.

Figure 9a shows the raised edge of the belly band indicating primary fracture occurred at the corner of the belly band and followed a path at an angle oblique to the surface of the sphere. Exactly this mode of failure was observed in cold compaction tests of spheres using Gd_2O_3,[1] supporting the concept of excess stress concentration in the equatorial plane generated by the higher effective pressures of the PuFF hot pressing mode.

Figure 10 compares the microstructure of the dense belly-band region with that of the less-dense polar region. The density of the belly-band region is so high that the identity of individual shards is almost obliterated and very few coarse pores remain. The polar region, on the other hand, is less dense, has a microstructure of partially discernible shards with more coarse intershard pores, and has fewer cracks.

Figure 11 shows microstructural defects in Sphere 1 which are typical of those observed in oxidized high-density PuO_{2-x}:[2] grain-boundary separations, microcracks, restructured intragranular image porosity, and intragranular cracks at the interface between γ-PuO_2 and eutectoid areas. Other defects include apparent gas-bubble precipitation in the grain boundaries. Since the aging time between hot pressing and heat treatment was so short, the bubbles cannot be attributed to helium. CO_2 gas is a possible explanation if the heat-treatment temperature was high enough (>1500°C).[2] The grain size of 25 μm (Table 3) is much larger

than the 8 to 10 μm expected for a proper density at 1440°C (Figures 3 and 4 of the July 1976 report,[6] and Reference 4). Even for the higher density of Sphere 1, the large grain size indicates heat-treatment temperatures may have exceeded the desired temperature by as much as ∿70°C.

The microstructures of all three pieces showed considerable heterogeneously distributed metallic impurities believed to be stainless steel and furnace refractories (p. 13 of the May 1974 Report[7] and p. 10 of the July 1974 Report[8]). A stainless steel vial in which the shards were transported had to be sawed open when the threads siezed. Steel particles were known to have been introduced into the shards.

Sphere 5 (Heat Treated)

Figure 12 shows the as-polished cross sections of an equatorial piece and a core piece of Sphere 5 chosen from among several pieces present after post-hot-pressing heat treatment. The piece believed to be part of the core appeared to be an edge piece because of the apparent curved exterior shown in Figure 12 and the existence and orientation of the cracked-uncracked regions. However, no spherical surface was noted when the piece was examined on the scanning electron microscope before mounting and grinding, and all surfaces had the appearance of a typical annealed fracture surface.[1]

The structures in Figure 12 are believed to show the microstructural characteristics across the interface of the highly fractured kernel observed regularly within fractured PuFF spheres (November-December 1977 report[1] and Figure 4 of this report). Both pieces exhibit a highly macrocracked region adjacent to a considerably less macrocracked exterior. The macrocracks are arrayed in networks typical of those in Sphere 1 and in $^{239}PuO_2$ pellets fractured by oxidation at densities above 85% TD.[2]

The overall densities of the pieces measured by mercury immersion were 86% and 84% TD for the equatorial and core pieces, respectively. Because these densities include an appreciable volume of internal cracks, the actual densities are considerably above 85%, and, hence, invited fracture on oxidation. The actual metallographic densities excluding macrocracks were measured as an average of several areas at 750X and are reported in Table 3 as 92% and 89% for equator and core, respectively.

Higher equatorial density is consistent with higher stress concentration in the belly-band. Figure 12 shows the equatorial piece was fractured on one side of the belly band and a deep radial fissure on the other side of the belly band.

Some of the general observations made for Sphere 1 can be made for Sphere 5, based on Figures 13 to 18. The shard identity had been destroyed indicating high pressure had degraded shards during compaction (Figures 13 and 16). the microstructures show a highly sintered condition and excessive grain size indicating excessive post-hot-press sintering temperature (Figures 15 and 18). The micro- and macrocracked surfaces are annealed, rounded, and sometimes even-healed, indicating the fractures occurred before or early in the post-hot-press heat-treatment (Figures 13b and 16b). No impurities were observed in the microstructures.

Properties of the Central Kernel

The higher magnification micrographs in Figures 13 to 18 show the contrast between the properties of the heavily macrocracked kernel and the less-macrocracked surrounding (exterior) region. These and other photomicrographs were used to determine the variation in grain size, density, and pore sizes given in Table 3. During sintering, at least two of the three properties — grain size, density, and pore size — increase concurrently as indicated in Table 3. Grain size and pore size are both larger within the kernel for both core and equator (Figures 15 and 18). However, densities excluding cracks did not change significantly. Grain size and porosity (size and number) changed discontinuously at the kernel interface over a distance of about 1 mm and were relatively constant within the respective regions.

The observation of a sharp transition region (at about 5% of sphere radius) in which both fracture and sintering features change discontinuously is reminiscent of a similar observation in $^{239}PuO_2$ pellets heat treated at 1530°C.[2] In those pellets, the central region was macrocracked in the same manner as in Sphere 5, but, unlike Sphere 5, the grain size was unchanged while the pore size and density were greater in the heavily macrocracked center. The cause then was speculated to be gas pressurization from residual trapped CO_2 in the high-density interior region. Densities in Sphere 5 are comparable to those in the $^{239}PuO_2$ pellets, although the as-pressed density distribution from surface to center is unknown for Sphere 5. The major difference between conditions experienced by Sphere 5 and the $^{239}PuO_2$ pellets is the temperature gradient in Sphere 5 resulting from self heating by ^{238}Pu alpha particles. Temperatures inside Sphere 5 were from 70°C to 200°C above the surface temperature depending on the nominal temperature of the sphere.

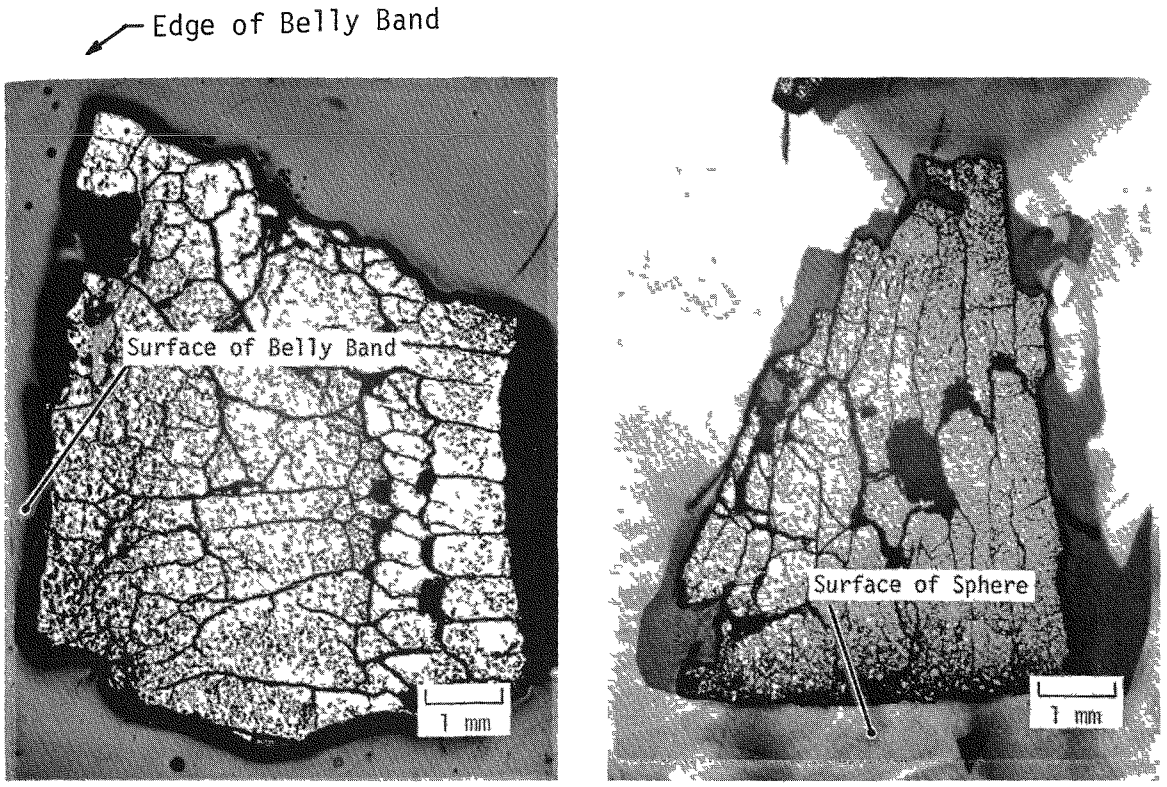

a. Belly Band

b. Pole

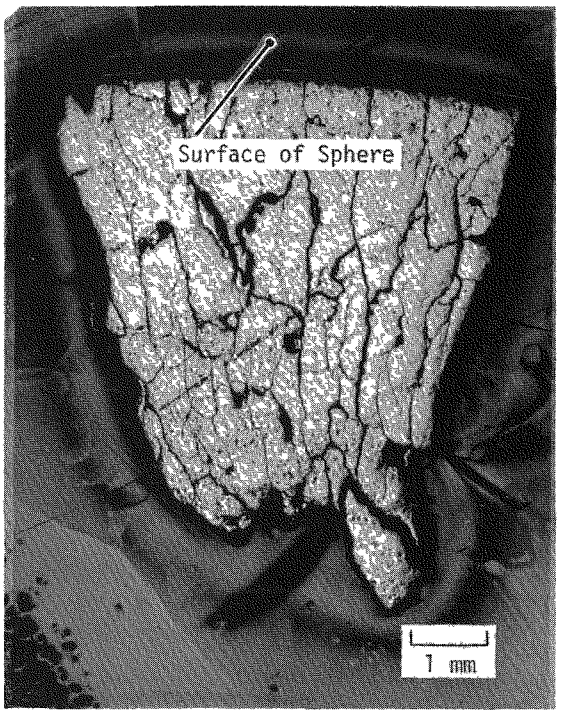

c. Random Section

FIGURE 9. Sphere 1 Heat Treated After Hot Pressing. (As-Polished).

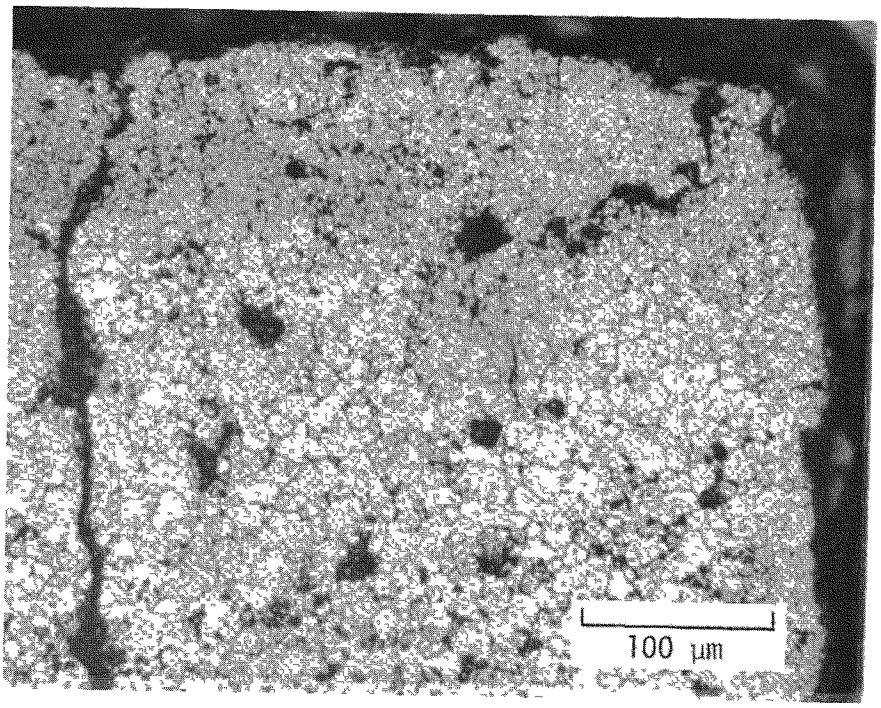

Equator at the Belly Band

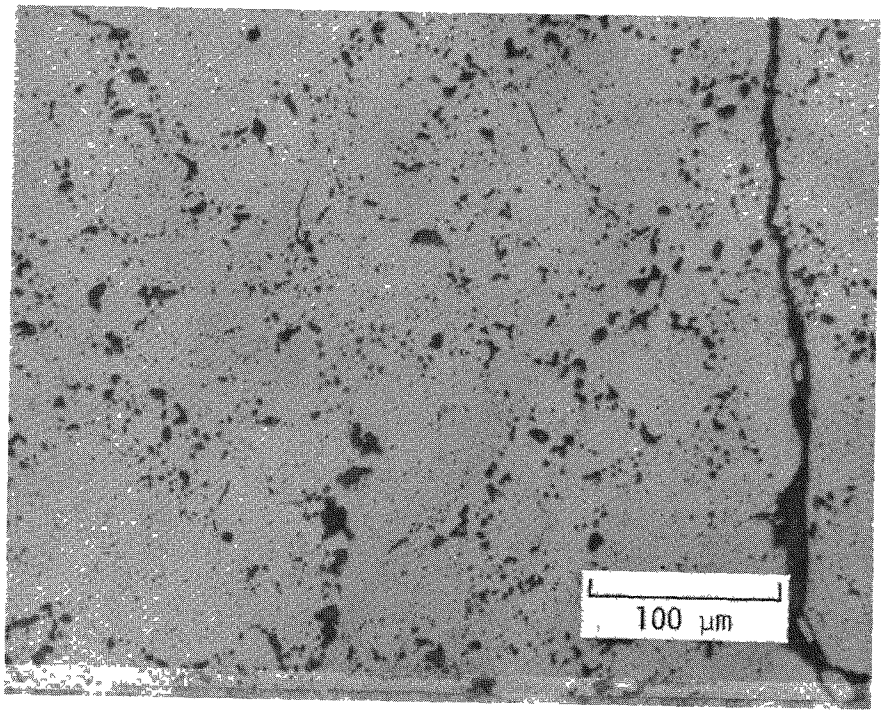

Pole

FIGURE 10. Microstructures of Sphere 1

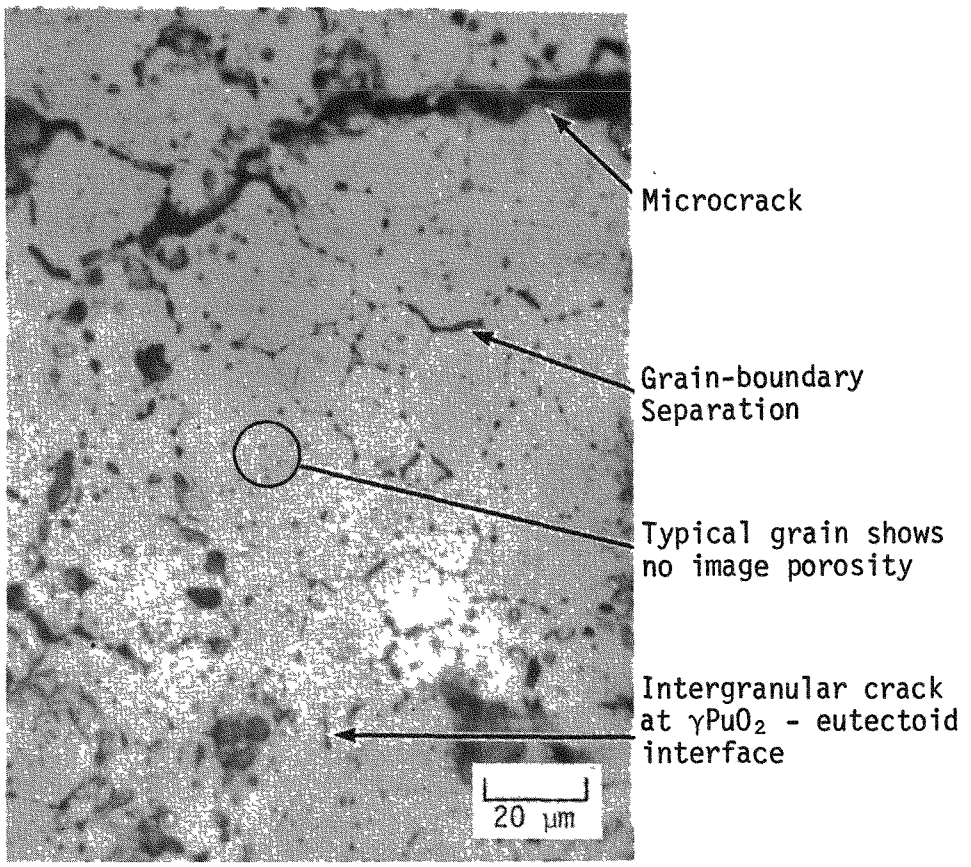

FIGURE 11. Sphere 1, Etched Microstructure of Belly Band Region

TABLE 3

Grain Sizes and Densities in Sphere 5

	Equatorial Region		*Core Region*	
	Fractured	*Less-Fractured*	*Fractured*	*Less-Fractured*
Grain Size				
Average Grain Size, μm	26	20	23	15
Expected Grain Size, μm	8 to 10		~10	
Inferred Temperature, °C	1575	1510	1530	1460
Difference, °C	65		80	
Density (Cracks at >85% TD)				
Metallographic Density,[a] % TD	92	92	89.5	88
Required Density for Observed Grain Size if 1440°C, % TD	97 to 98		95	
Immersion Density, % TD	86		84	
Pore Size	Larger	Smaller	Larger	Smaller

a. Excluding cracks.

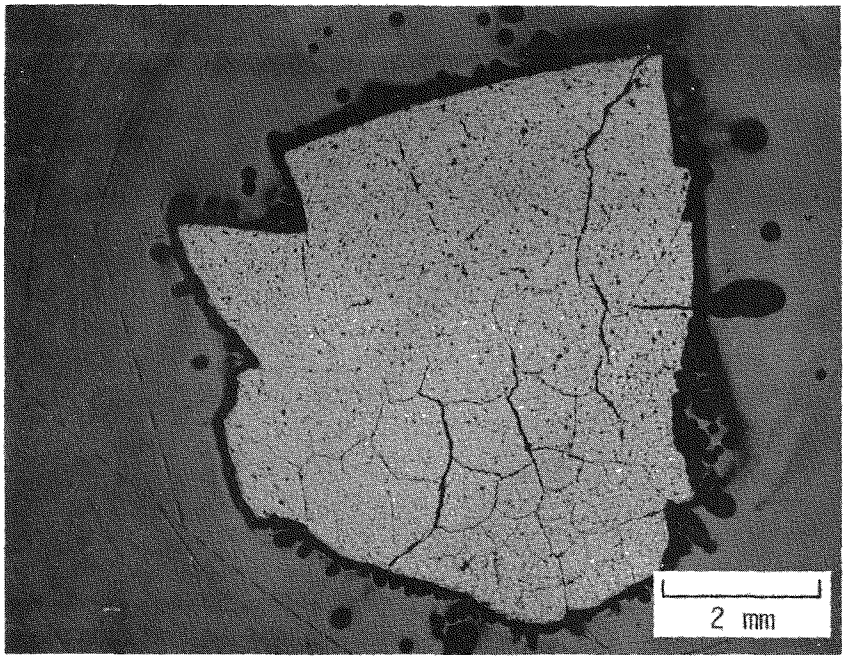

Core

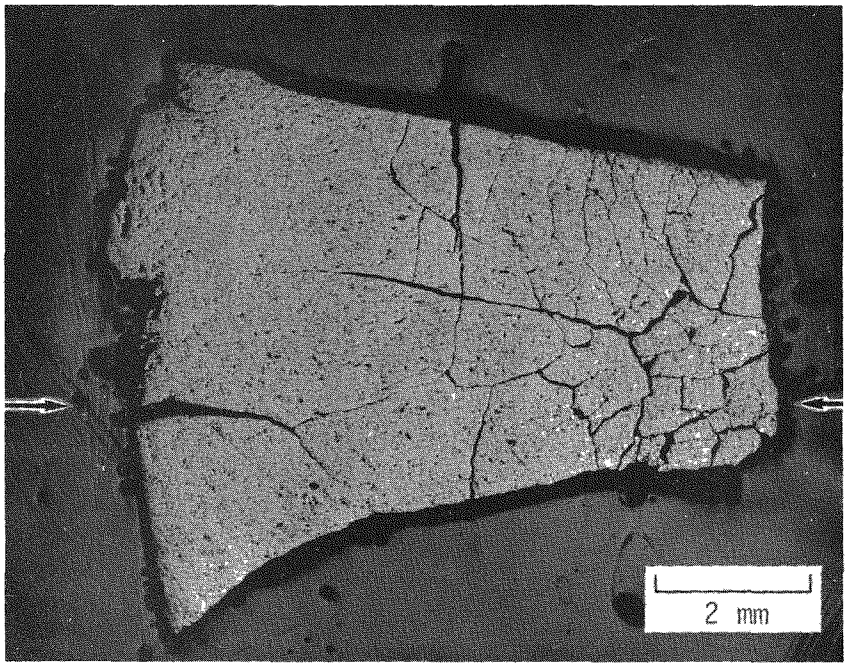

Equator at Belly Band

FIGURE 12. Sphere 5 Heat Treated After Hot Pressing. (As Polished).

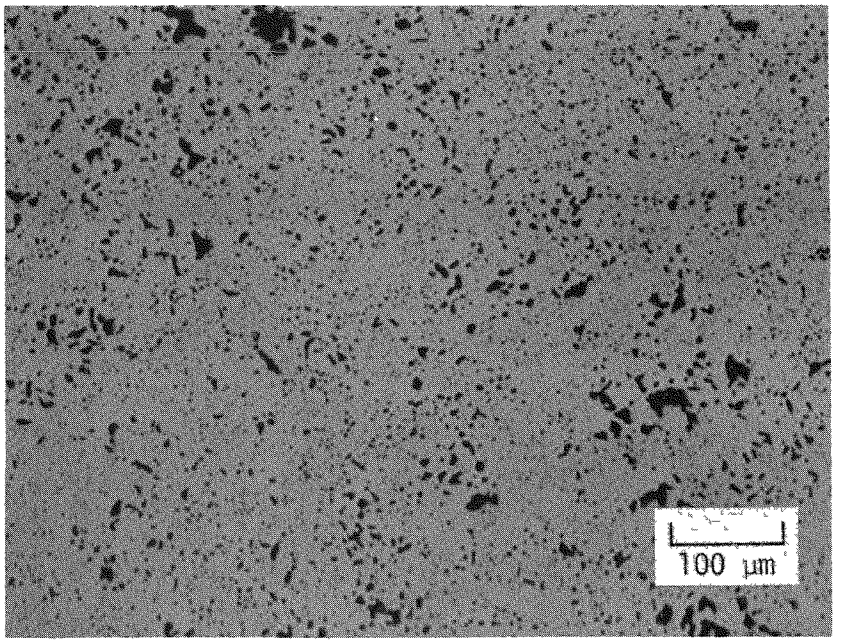

a. Shell

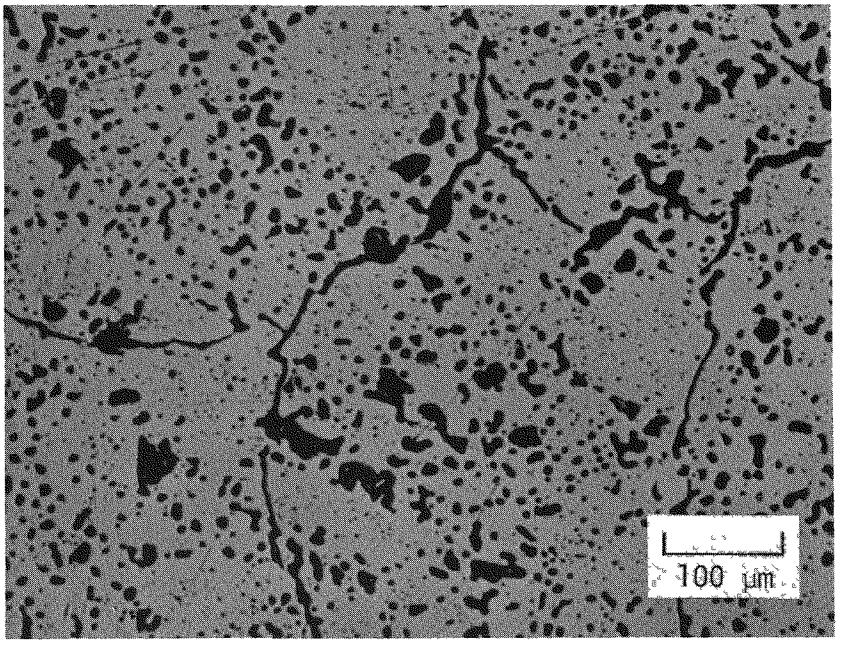

b. Cracked Kernel

FIGURE 13. Core of Sphere 5

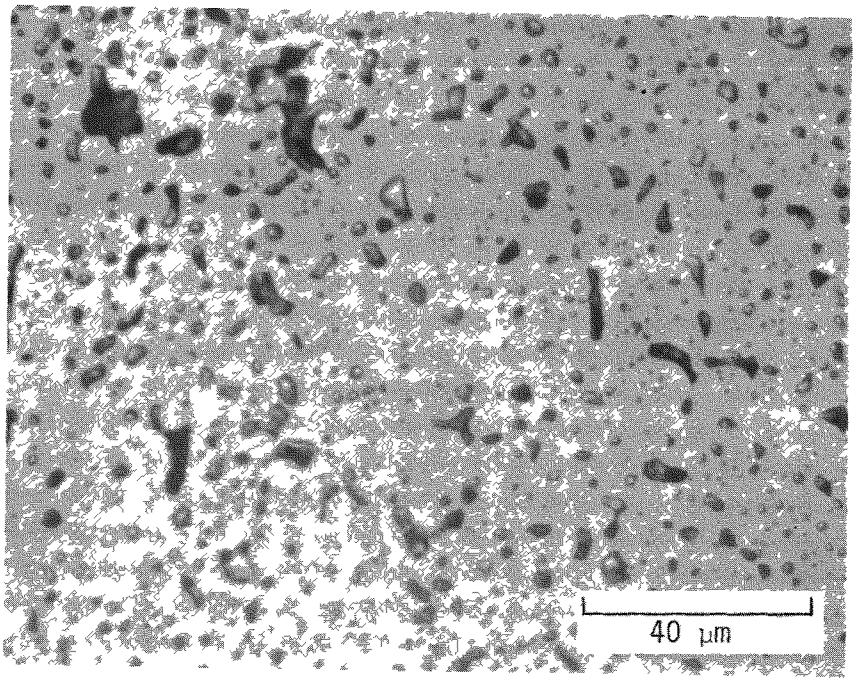

Shell

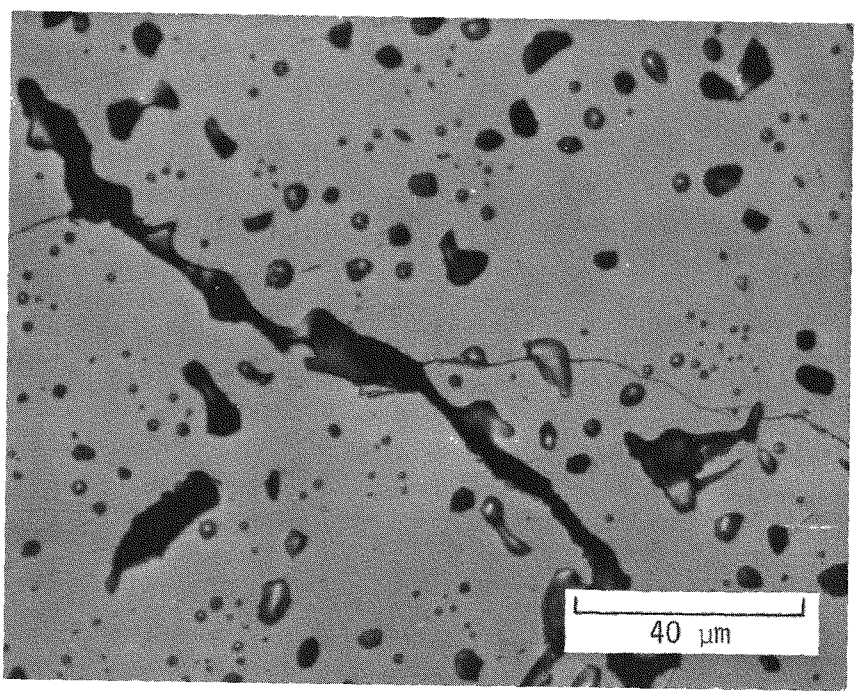

Cracked Kernel

FIGURE 14. Core of Sphere 5, As Polished

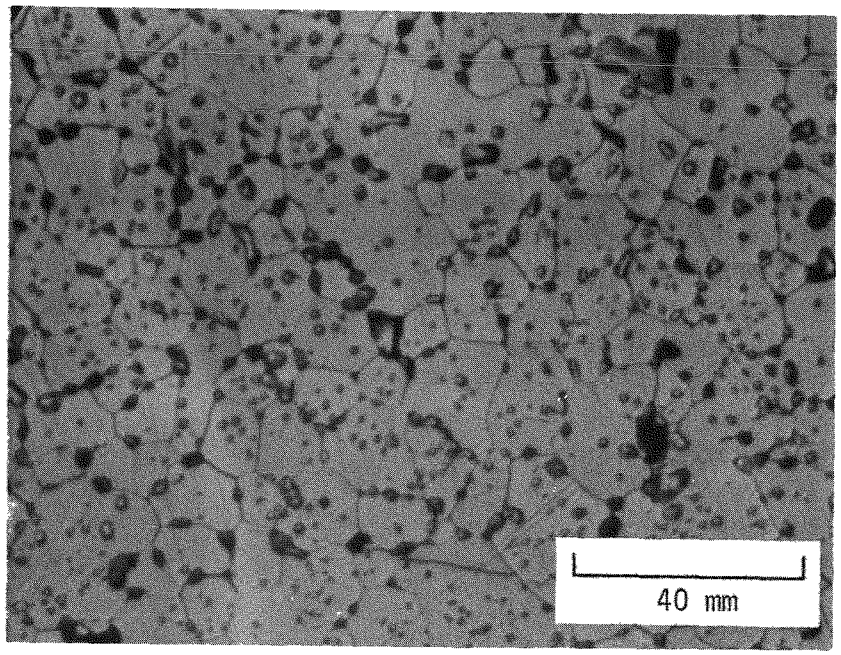

Shell

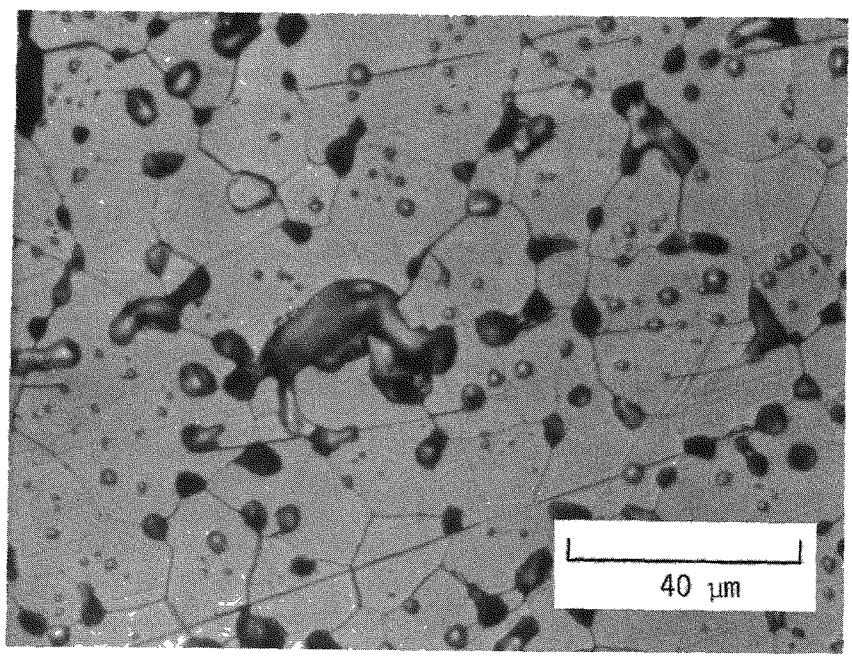

Cracked Kernel

FIGURE 15. Core of Sphere 5, Etched for Grain Boundaries

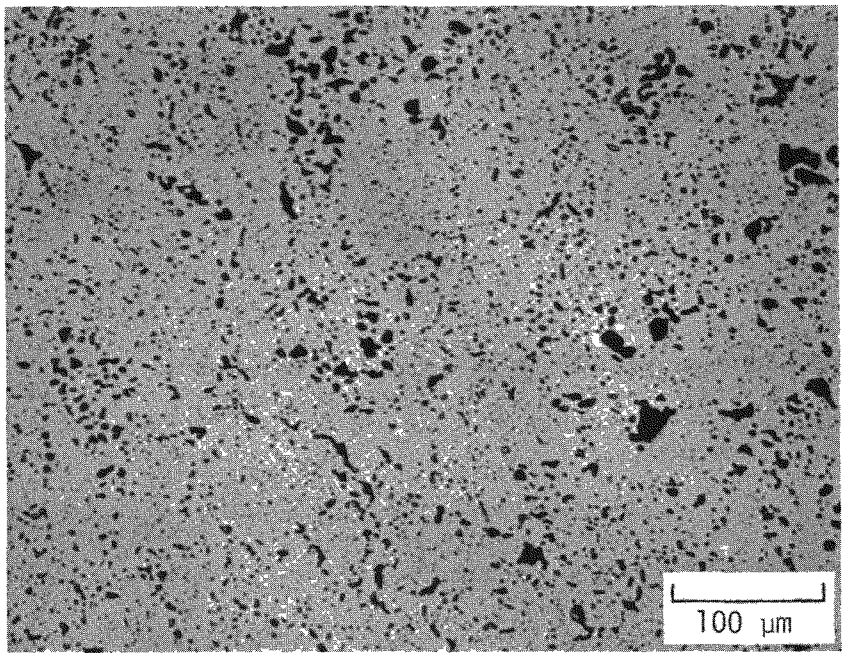

a. Shell

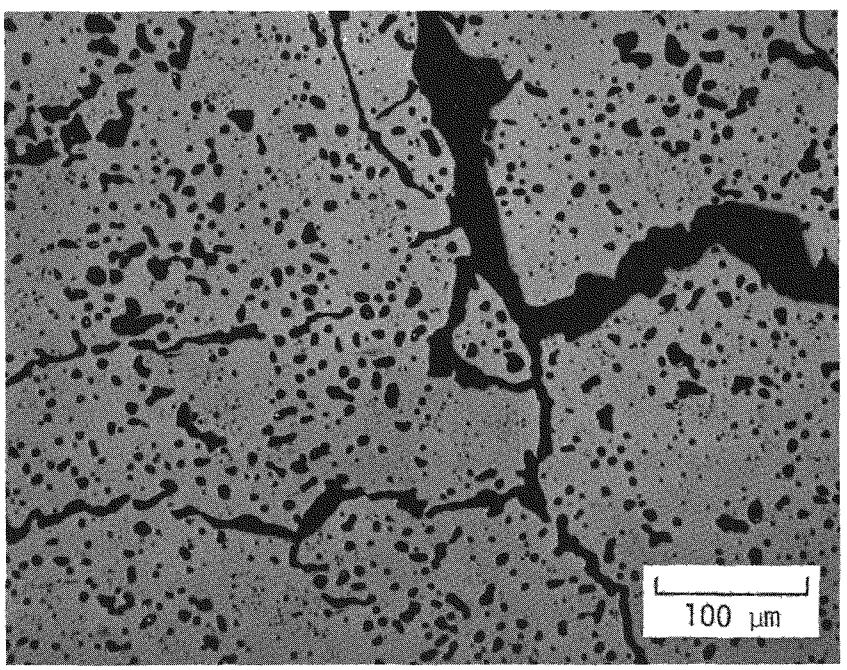

b. Cracked Kernel

FIGURE 16. Equator of Sphere 5. (As-Polished)

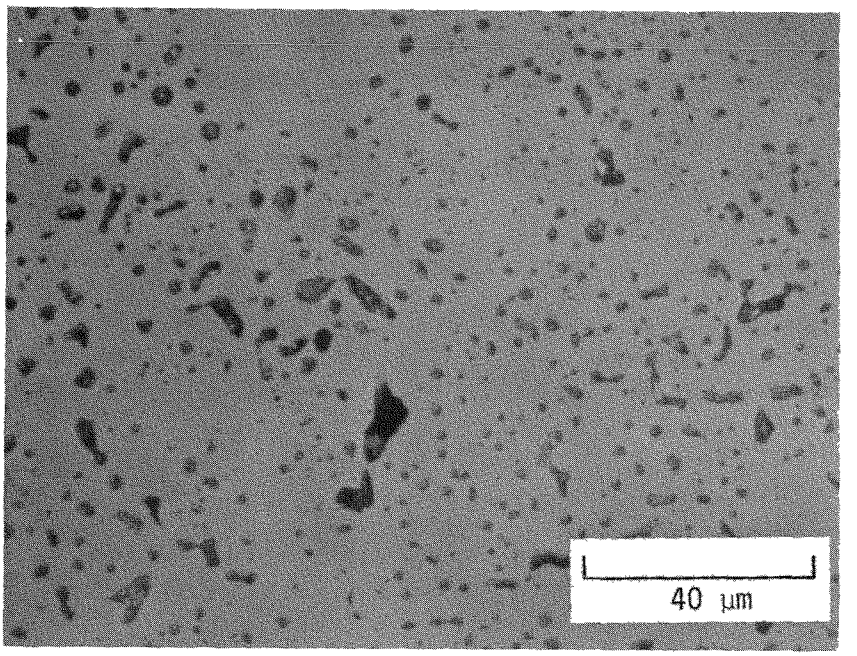

Shell

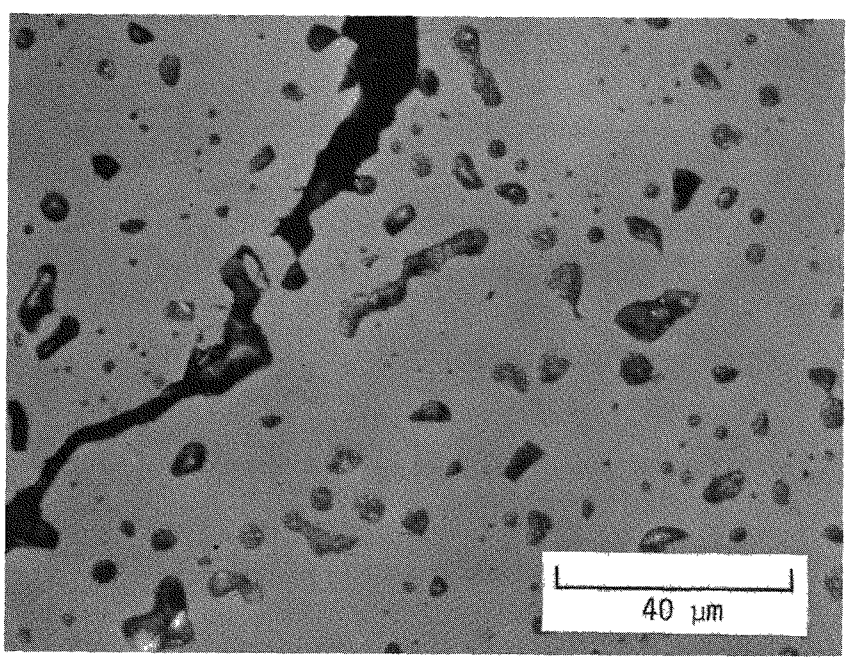

Cracked Kernel

FIGURE 17. Equator of Sphere 5. (As-Polished)

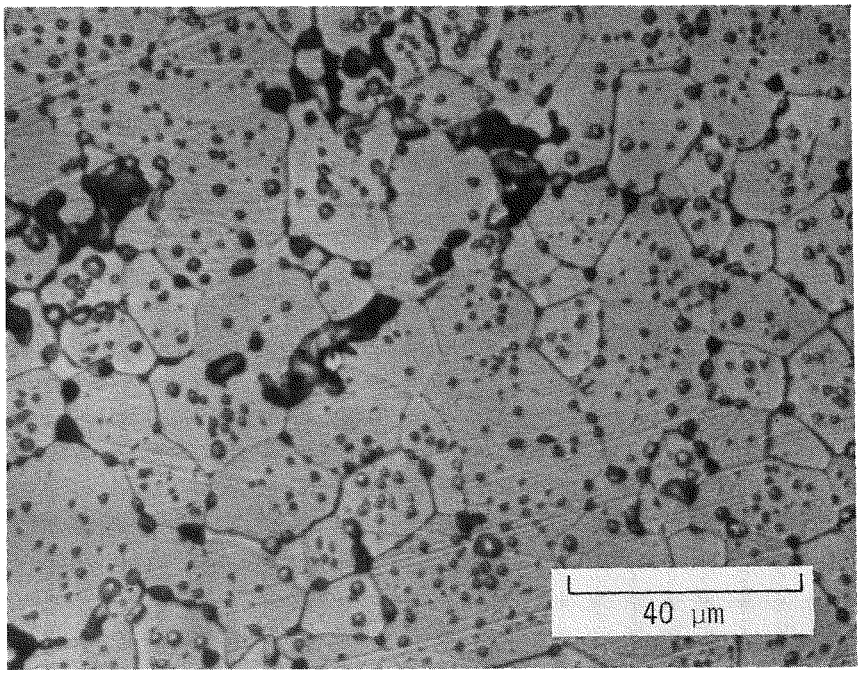

Shell

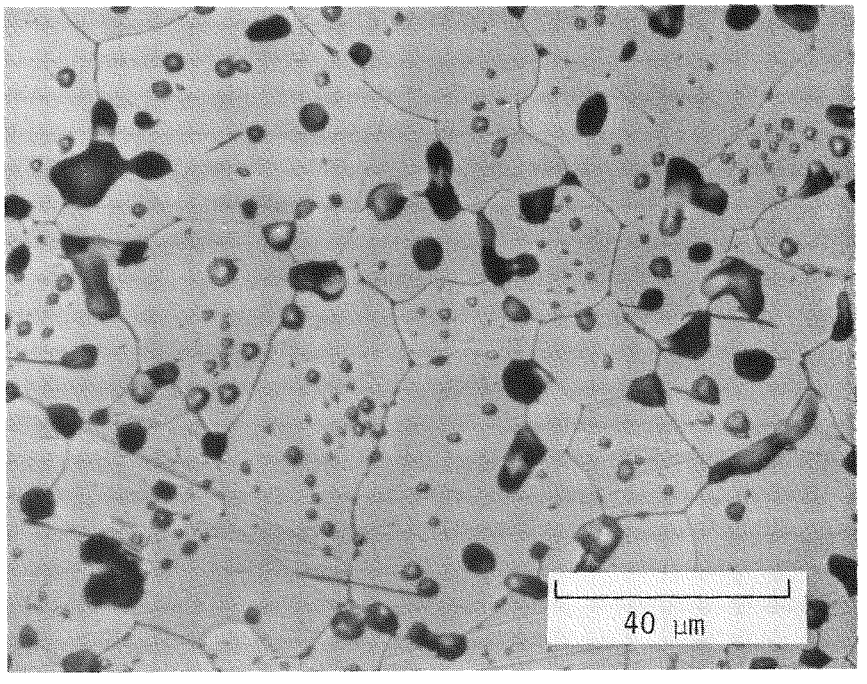

Cracked Kernel

FIGURE 18. Equator of Sphere 5. (Etched for Grain Boundaries)

The existence and characteristics of the kernels in heat-treated spheres with sharp interfaces to the surrounding exterior region may be caused by temperature, O/Pu, and carbon gradients formed during hot pressing by density, and by subsequent temperature and temperature gradients during reoxidation, all acting in concert to create high CO_2 pressures concentrated toward the center of the sphere. Because densities, excluding macrocracks, across the kernel interface varied insignificantly (Table 3), differential sintering effects associated with regions of different densities cannot alone explain the cause of severe cracking of kernels. A gas-induced fracture effect apparently does have a fairly sharp temperature dependence, occurring between 1370 and 1530°C in the earlier $^{239}PuO_2$ test,[2] which may account in part for the discontinuous change in macrostructural features across the kernel interface. LASL recently noted significant changes in diffusion-dependent properties of PuO_2 between 1400 and 1500°C in mechanical property tests.[9] Temperatures in this range are attained during both hot-pressing and heat treatment. With the surface of the sphere at 1490°C during hot pressing and 1440°C during post-hot-press heat-treatment, the interior of the sphere would increase radially in temperature to about 1560°C and 1510°C, respectively, at the center.

A temperature threshold phenomenon in the above temperature range at densities near 90% TD or above could produce an interior region of different behavior whose volume depends both on the extent to which CO_2 that was formed on oxidation can escape from the surface and on the temperature where vacancies can diffuse so that porosity can redistribute. Reduction of the PuO_2 sphere during hot pressing must occur to a greater extent in the interior of the sphere because of the temperature gradient. At constant pressure of CO, CO_2, and O_2 in the die cavity, the higher-temperature center is reduced more than is the surface, establishing a composition gradient. Consequently subsequent oxidation is accompanied by a larger volume decrease and higher resulting stresses in the central portion than in the surface region of the sphere.

Such a composition gradient during hot pressing should be gradual and should not show such a sharp change in properties as represented by the kernel in Sphere 5. However, the central portion would also contain more carbon. On cooling in the hot press, lower O/Pu compositions toward the core will have a greater potential to reduce residual CO gas than will higher relative O/Pu compositions nearer the surface. Under these different reducing conditions, there would be a higher potential for increased fracture in the kernel because of CO_2 gas evolution during post-hot-press heat treatment at temperatures near 1500°C. Thus, the kernel interface is relatively sharply defined because of the compounding effects of temperature gradient, composition

gradient, carbon concentration gradient, and temperature for diffusion of vacancies to grain boundaries. The changes in grain size and pore size of $^{238}PuO_2$, rather than density and pore size as in $^{239}PuO_2$, may be attributed to gradients of temperature and O/Pu ratio occurring in $^{238}PuO_2$ fuel forms.

Whatever the cause of the severely cracked kernels, pressing to lower densities (<85% TD) is expected to eliminate such kernels.

Excessive Post-Hot-Press Heat-Treatment Temperature

The grain sizes listed in Table 3 are too large for the observed density, indicating the post-hot-press sintering temperature may be as much as ∿70°C too high; this is consistent with recently discovered inaccuracies in temperature measurement and corrections for the radiant heat from the sphere relative to the location of the thermocouple in the vertical heat-treatment furnace.

LASL[4] and SRL[6] have determined the expected grain size to be 8 to 10 μm for MHW spheres at 82 to 85% TD heat-treated at 1440°C. Table 3 shows considerably larger grain sizes than this, but also higher densities, which only partially explains the larger grain sizes. Grain growth occurs mostly during post-hot-press heat treatment at 1440°C for 12 hr, and very little during the short hot pressing period.

Table 3 shows that the 20-μm grain size in the Sphere 5 equatorial fragment for a metallographic density of 92% TD would require a heat treatment temperature of 1510°C, or 70°C above the nominal heat-treatment temperature.[10] Alternatively, if the temperature were 1440°C, the 20-μm grain size would require a density of 97 to 98% TD which is, of course, considerably higher than the 92% TD observed. Similar measurements and calculations for the core piece imply a temperature too high by about 20°C or a density discrepancy of 3%. The temperature difference inferred from the grain-size differences between the fractured center and less-fractured surface in both pieces is approximately the expected ΔT 60 to 80°C between the surface and center of the sphere at 1500°C (Table 3). The difference is 65°C in the equatorial piece and 80°C in the core piece.

Sphere 4 (Not Heat Treated)

An equatorial piece and a polar piece were selected from among the fragments of Sphere 4. This sphere was not heat treated after hot pressing. The sphere was hot pressed to a nominal 86% TD; it cracked at ambient temperature during exposure to oxygen impurity in the argon cell gas, and it fractured when it was dropped.[1]

The structures of as-polished cross sections are shown in Figure 19. Both pieces show considerably less macrocracking than in the heat-treated spheres consistent with oxidation under less-agressive conditions and lower densities (see below). However, micro- and macrocracks do exist. As in Spheres 1 and 5, the equatorial piece is more dense than the polar piece and contains more macrocracks. The micro- and macrocracks are thin and sharply defined, indicating they were formed at low temperature.

The polar piece fractured along radial cracks typical of the three macrocracks shown in Figure 19. These radial cracks are spaced about 1000 μm apart, about the same as those observed in Sphere 1. Again the spacing of such surface cracks perpendicular to the exterior surface is typical of that observed in $^{239}PuO_2$ pellets oxidized between 600 and 1100°C.

The polar piece exhibits three distinct zones of different microstructures (Figure 19). These zones are shown at higher magnification in Figure 20. The sphere surface at the pole shows a normal MHW density (83% TD) with a structure made up of distinct shards and containing no microcracks. The depth of this zone is 3 to 4 mm, which is typical of the thickness of the low-density polar layer observed in ink penetrant tests of cold-pressed simulant spheres.[1]

Zone 2 is the highest-density zone and has microstructures similar to those observed in the sections of Spheres 1 and 5 described above. This zone contains considerable macro- and microcracks. Zone 3 has a microstructure intermediate between the microstructures of Zones 1 and 2 (Figure 20). These observations indicate a poor distribution of pressing forces during compaction of the sphere.

Figure 21 shows other features of the polar section. Grain-boundary separations were observed, particularly within the shards of Zone 3. these separations are similar to those observed after oxidizing $^{239}PuO_{2-x}$ pellets.[2] Microcracks and grain-boundary separations were observed in the zone of highest density, Zone 2. Fully dense rectangular pieces were observed frequently in Zone 1 where the density contrast with shards made them discernible. Such pieces have been observed and reported before, particularly in pellets made with powder milled at SRL, and are attributed to flakes of compacted powder created when mill jars are scraped after milling.

Figure 22a shows the typical microstructure in the equatorial piece. The structure is quite dense, as in Spheres 1 and 5, and relatively uniform throughout the piece. Shards are not identifiable. Macro- and microcracks are both present. These observations support the excessive densification in the equatorial region and cracking in high-density areas because of oxidation.

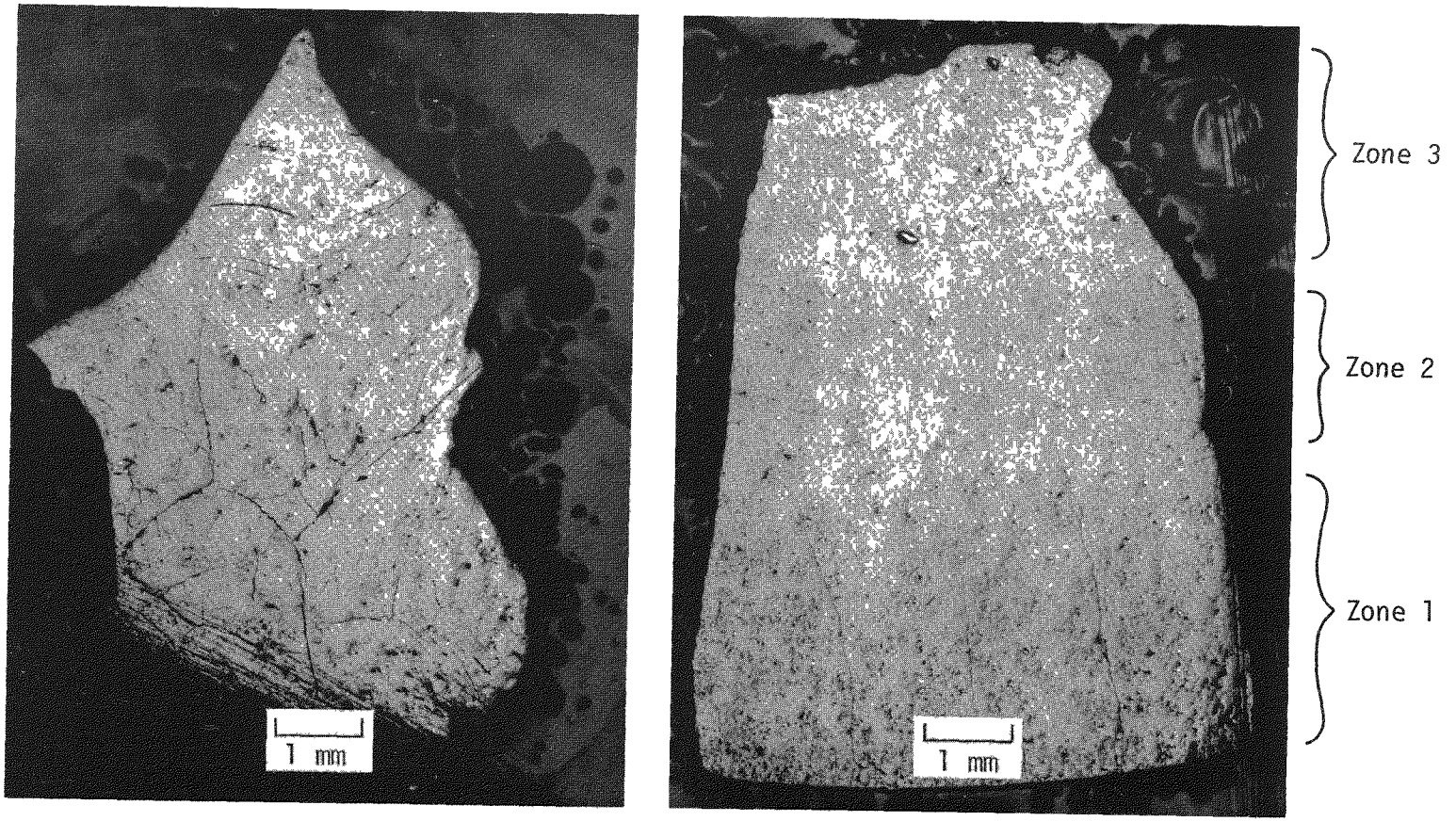

FIGURE 19. Sphere 4, Not Heat Treated After Pressing. (As-Polished.)

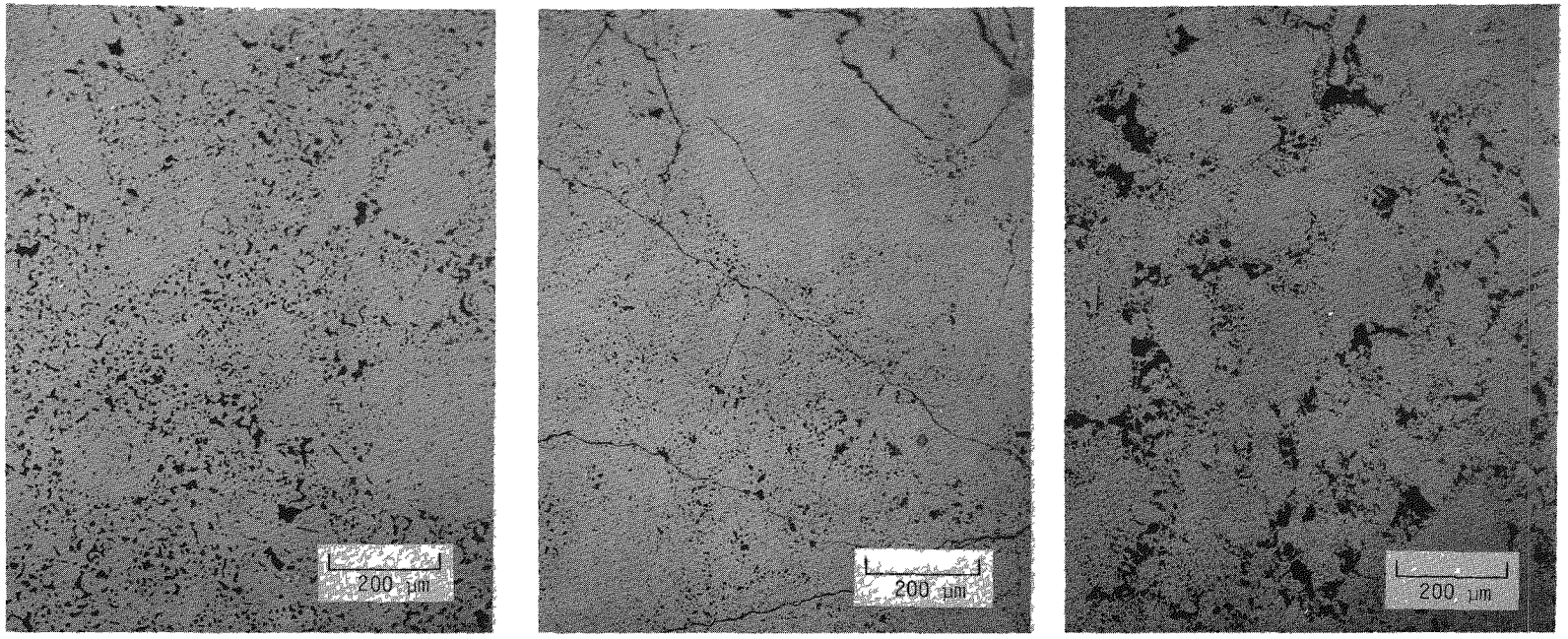

Zone 3 Zone 2 Zone 1

FIGURE 20. Microstructural Variation and Crack Incidence in Polar Piece of Sphere 4. Not Heat Treated After Pressing. (As-Polished)

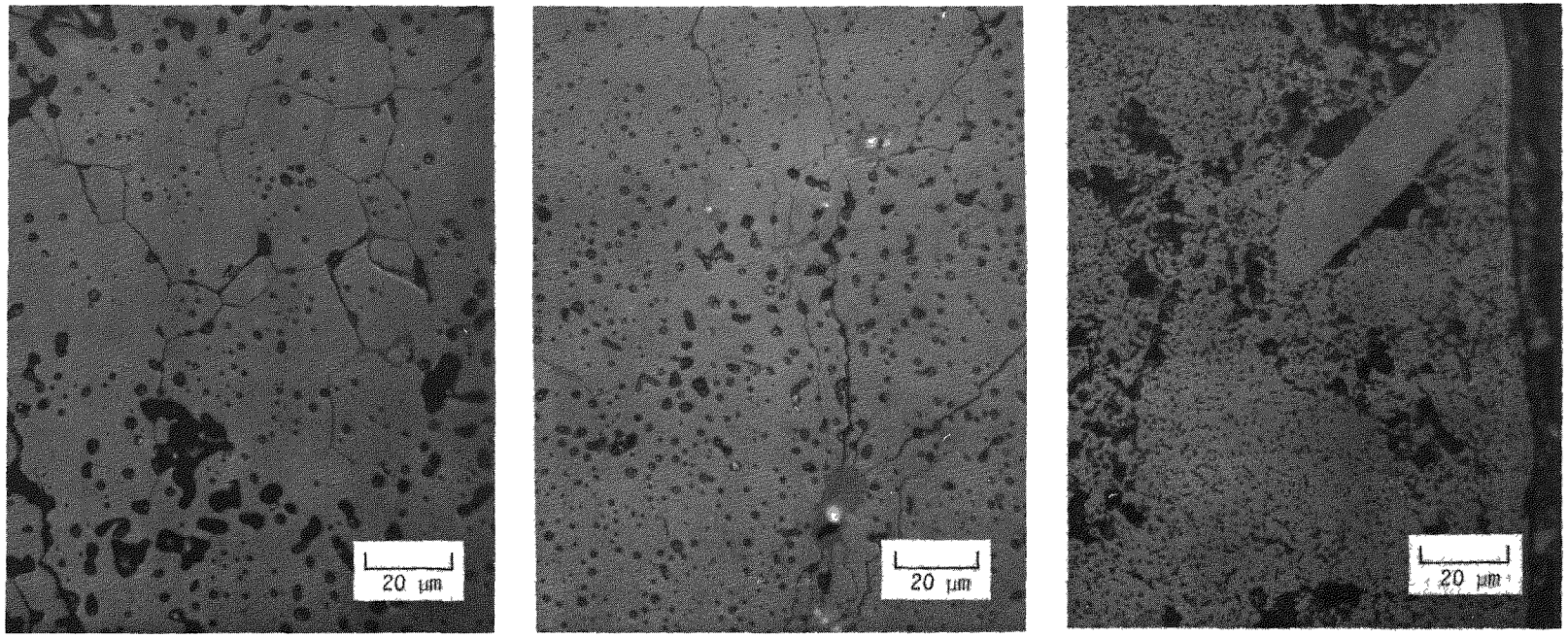

Zone 3
Grain-Boundary Separation

Zone 2
Microcracks in Grain Boundaries

Zone 1
High-Density Rectangular Shards

FIGURE 21. Sphere 4. Microstructural Aberrations in Polar Piece. Not Heat Treated After Pressing. (As-Polished)

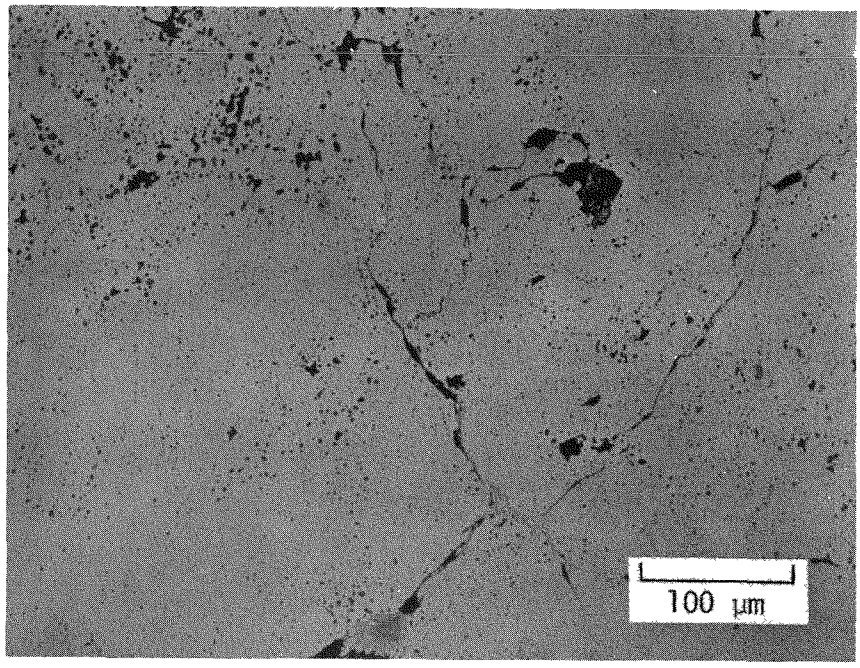

a. Typical Density and Macrocracks

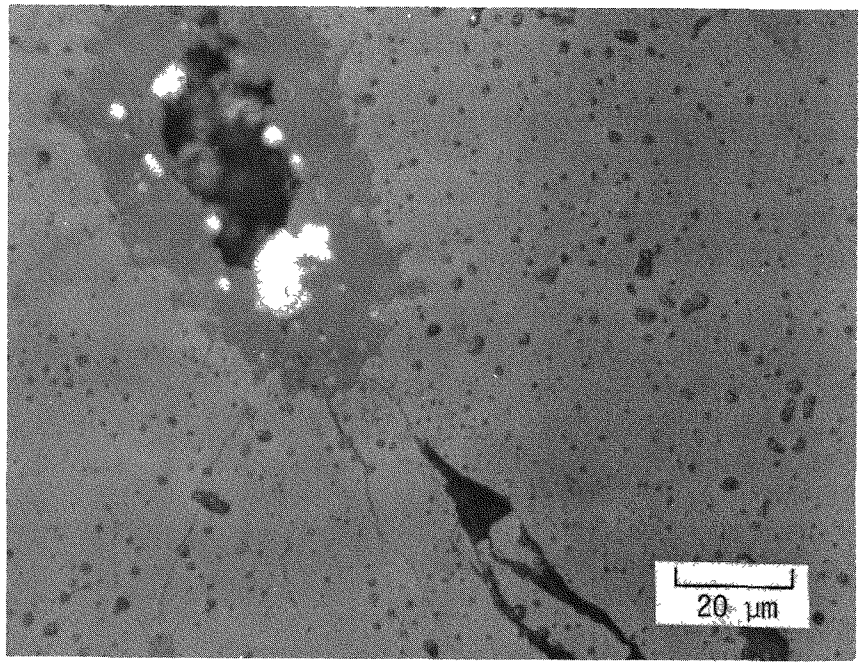

b. Impurities in Cracks

FIGURE 22. Sphere 4. Equatorial Piece. Not Heat Treated After Pressing. (As-Polished)

Both pieces of Sphere 4 contained considerable impurities, believed to be stainless steel and furnace refractories. The impurity concentration was higher than observed in Sphere 1. These impurities are shown in Figures 21 and 22b. The grain-boundary separations and cracks are associated extensively with these impurities suggesting that the impurities may have contributed to the formation of these defects. The appearance of the impurities is identical to that observed in pellets and reported previously.[7,8] Analyses of those impurities revealed that they were Fe, Cr, Ni (stainless steel) in the light metallic-appearing areas and Al, Ca, Mg and O (furnace refractories) in the gray areas.

PARAMETRIC STUDIES IN PuFF

As previously described (November-December 1977 report[1] and this report), Spheres 1 to 10 were for the most part undersized, too dense, and highly cracked or fractured. Evidence from analyses and previous tests indicates excessive application of hot-pressing pressure is the prime reason for the inferior product; shard quality (strength and sinterability) may be the next most important factor.

Effects of hot-pressing pressure application were described above in detail. SEM Analyses of the shard batches made in PuFF for the first nine spheres (Figure 23 of this report and Figures 11 and 12 of the November-December Report[1]) indicate a large variation in size and size distribution among batches even though they were made under nominally identical conditions. This variation in shards probably led to some variation in pressing behavior, as illustrated in Table 4 for pairs of spheres hot pressed under similar conditions. However, the amount of variation attributable to hot-pressing variability and the amount attributable to shard variability is unknown.

TABLE 4

Variability in Dimensions of As-Pressed Spheres

Sphere Pairs	*Temp of Pressure Application, °C*	*Final Temp, °C*	*As-Pressed Dimensions, in.*	
			Equator	*Pole*
4	1350	1420	1.459	1.447
5	1370	1525	1.469	1.463
5	1370	1525	1.469	1.463
8	1260	1550	1.452	1.450
6	1470	1495	1.453	1.459
9	1490	1520	1.463	1.472

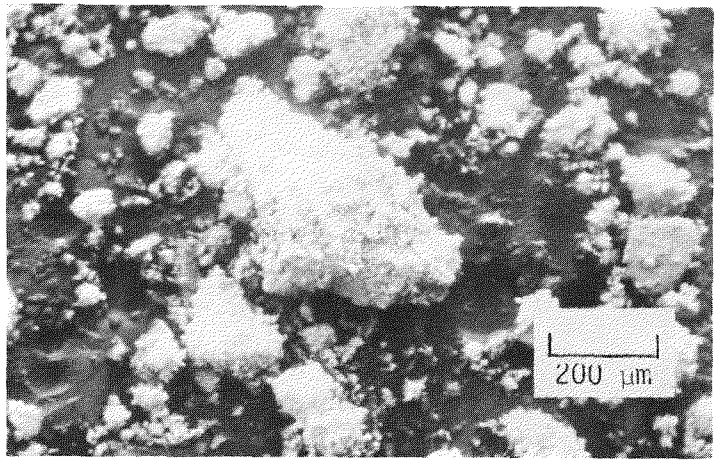

Sphere 4 Shards

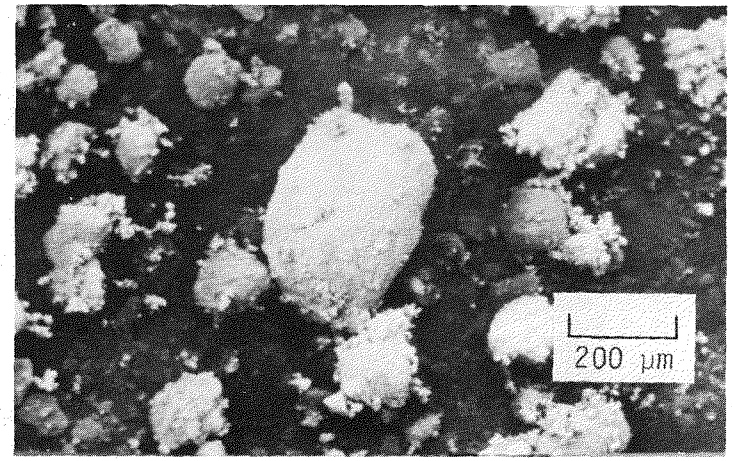

Sphere 8 Shards

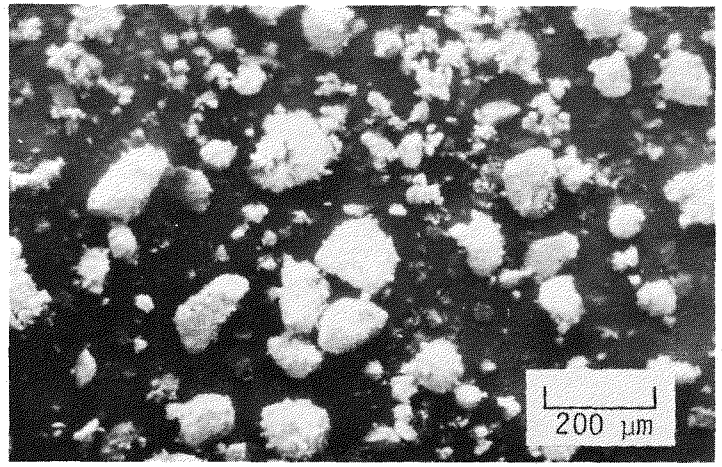

Sphere 6 Shards

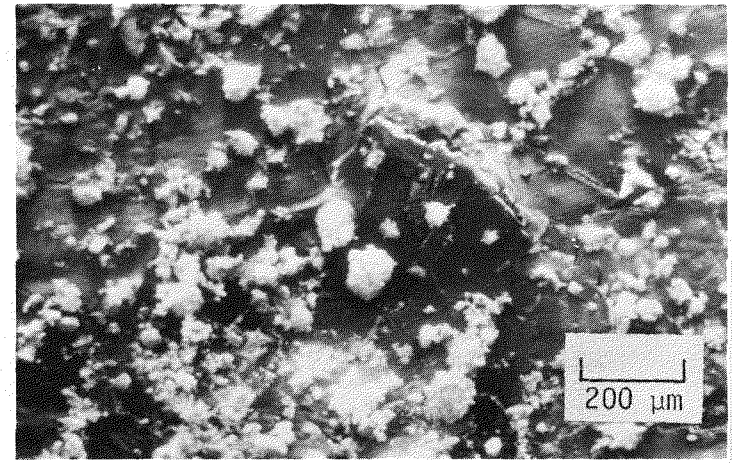

Sphere 9 Shards

FIGURE 23. SEM Analysis of Shards for Spheres 4, 6, 8, and 9

The parametric experiment for the PuFF Facility will investigate how shard characteristics and the important processing steps affecting shards, and how hot-pressing conditions affect the quality of heat-treated spheres.

Reasons for Systematic Parametric Studies

The LASL flowsheet has not reproduced LASL-type shards and acceptable spheres in the PuFF Facility because of at least three general conditions:

- Major equipment differences between PuFF and LASL, such as design of hot-press die tooling, process furnaces, and ball mill.

- Unavoidable differences in handling, even though the process steps are nominally the same. Handling differences arise mainly because PuFF is designed as a production facility, with remote manipulation, whereas LASL is not.

- No limits were established on the process variables by LASL.

The best way to evaluate the impact of these conditions and to tune the process for PuFF operation is with a statistically designed experiment, called either a parametric or matrix study. Such a study is currently being applied to the production of shards in PuFF and has as its primary objective the determination of a suitable centerline flowsheet. The study is designed to evaluate a large number of variables and to determine those variables for which the process is most sensitive and those which are not particularly important. The parametric study ranks the significant variables in order of importance and provides information on the practical limits for each variable. The limiting conditions used in the parametric experiment will form the basis for limits for the Technical Standards.

Description of PuFF Parametric Studies

A Plackett-Burman statistically designed study was selected to evaluate important processing variables. The process steps selected for the parametric study are given in Table 5. Because of time constraints, the size of the test matrix was limited to the parameters given in Table 5. Variables were chosen on the bases that (1) the operation is likely to have a large effect; (2) the operation is a major source of process variation but has an uncertain effect; or (3) process control is difficult. A brief description of each variable follows.

- Feed powder (size and shape), mill style, mill charge, and mill time all affect the size (size distribution) and shape of the milled powder. Size and shape, in turn, affect compaction behavior in the cold press. Compaction behavior in the cold press affects breakup during sharding, shard density, and shard sintering behavior (grain growth). Finally, shard characteristics affect compaction during hot pressing and the resulting fuel microstructure.

- Post-ball-mill screening may break up agglomerates formed during milling and improve cold compaction. If there is a significant effect between screen sizes, it should be maximized by screening or not screening.

- The cold-press pressure is easy to control. In addition, cold-pressed density is not a strong function of pressing pressure at the high pressures being used. Therefore, cold-press pressure was not included as a variable.

- The two actions used for sharding — brushing or rolling the cold-pressed pellet through 300-μm and 125-μm screens — have a large potential for producing variations in the shards. Brushing is a more-severe action than rolling and might be expected to abrade and round the shards, producing a different shape and more fines than rolling. The relative amount of use of one or the other action may also vary significantly among shard batches for any one operator doing the work as well as among operators.

- Allowing or not allowing the unfired shards to stand for at least 12 hr before sintering was included as a variable to test the effect of production delays. There are many opportunities for interruption of powder processing, and the question of powder degradation because of these delays has been raised. One of the correlations made for Spheres 1 to 10 is that Spheres 4 to 6 (generally considered the least successful spheres) were made using only day shifts and, therefore, had many delays between operations. In contrast, shards for the other spheres were made using shift work, where necessary, to maintain process continuity. The correlation may be coincidental, but delays can be a major source of variation. Delays at the sharding stage may not be equivalent to delays at other times, but this point was chosen because it was the point of delay most often encountered in making Spheres 1 to 10.

- Sintering temperature, in concert with powder operations, affects the density and, therefore, strength and sinterability of the shards.

- Effects of the hot-pressing variables were described previously.

TABLE 5

Parametric Study[a]

Variable	*Centerline*	+	-
Feed Powder - Particle Mode Size, μm	4-6	6.7 - 8.2 (Thick)	4.2 - 4.3 (Thin)
Mill Style	-	SRP (w/baffle) 100 rpm	LASL (w/o baffle) 27 rpm
Mill Charge, g	75	80	65
Mill Time, hr	12 (SRP)	14 (SRP)	8 (SRP)
	32 (LASL)	32 (LASL)	24 (LASL)
Post-Ball-Mill Screening, μm	300	300	125
Cold-Press Pressure, psi	58,000	0	0
Crushing Method	-	Brush Through	Roll Through
Allow Green Shards to Stand	-	Yes	No
Shard-Sintering Temp, °C	1175	1300	1150
Hot-Press Pressure, psi	-	3000	600
Pressure Application Rate, lb/min	-	Full Pressure in 10 sec	Full Pressure in 3 min
Hot-Press Temperature, °C	-	1550	1440

---

a. The study requires twelve runs to complete. Each run represents a different permutation of the variables.

Results of the parametric tests will be evaluated in the following manner:

- Visually analyze by SEM shard batches to demonstrate general variations in size and shape of the shards.
- Measure tap density of shards to determine relative flowability. This is related to the ease of uniformly compacting shards during hot pressing.
- Analyze the batches of powder by SEM and Coulter counter (particle size and size distribution) as necessary to determine crucial step(s) in producing good (or bad) shards.
- Hot press and sinter small pellets (18 g) from each of the twelve different shard batches.
  - measure the relative shrinkage between hot pressing and heat-treatment
  - measure the final density
- Perform metallography of hot-pressed pellets.

In addition to the parametric experiment involving the sharding steps, full-size spheres will be fabricated to verify the limits determined from the parametric study.

CONTROL OF MICROSTRUCTURAL DAMAGE PRODUCED BY HELIUM RELEASE IN 80%-DENSE $^{238}PuO_2$ PELLETS

Additional metallographic examinations of 80%-dense $^{238}PuO_2$ pellets heated after extended aging confirmed previous observations, viz, that insufficient helium was released below threshold temperature for microstructural damage to avoid grain separations caused by helium release above the threshold temperature (August 1977 report, p. 7[11]). Confinement of the grain separations to the interiors of the high-density regions of the pellets could not therefore be attributed to helium depletion at the edges by a subthreshold release mechanism, such as grain-boundary diffusion. The distribution of observed grain separations appears instead to be a basic characteristic of the network of interconnected channels formed above the damage-threshold temperature to release accumulated helium. Provision of microstructures with high-density regions no greater than about 25 μm should, however, avoid most of the grain separations. $^{238}PuO_2$ forms prepared by direct fabrication of a calcined Pu^{4+} oxalate feed might meet this requirement.

Temperature Dependence of Grain Separations

The current tests were conducted to confirm previous results establishing the temperature dependence for formation of grain separations in aged $^{238}PuO_2$ (August 1977 report, p. 7[11]). Specimens employed were segments from three 1/4-in.-dia. by 1/4-in.-thick $^{238}PuO_2$ pellets prepared in April 1975 and stored for 28 to 30 months near room temperature. Alpha decay over this time generated a helium concentration of about 1.7% of the Pu atoms. The pellets were fabricated from <125-μm oxalate-base $^{238}PuO_2$ shards by hot pressing in a multicavity die under 3000 psi pressure for 20 min at 1530°C in vacuum atmosphere, then heating at 1440°C for 12 hr in air (April 1975 report, p. 21[12]). Densities of the pellets after heat treatment were about 80.5% TD. Typical microstructures displayed high-density regions representing the original shards surrounded by large irregular pores as shown in Figure 24 (see also July 1975 report, p. 14[13]). Grain size in the high-density regions was typically <15-μm.

After storage, the pellets were sectioned into several segments and the segments were heat treated up to 4 hr in air at temperatures given in Table 6. Single-temperature treatments in the range 1000 to 1500°C were used to confirm the previously established temperature threshold of about 1200°C for grain separation caused by helium release. Duplex-temperature treatments were used to determine effects of preheating below this temperature threshold on microstructural damage subsequently incurred above grain-separation thresholds. In contrast to the previous tests, the specimens in the current tests were heated directly from preheat temperatures to final temperatures, without the intermediate cooling employed in the previous tests.

Microstructures of the specimens, shown in Figure 25, revealed no grain separations in specimens heated at 1000 and 1100°C. Specimens heated at 1200°C showed thin grain separations in a few high-density regions, while specimens heated at 1300, 1400, and 1500°C showed more-frequent, severe grain separations. In all cases, the observed grain separations were most pronounced in the interiors of the high-density regions, leaving a peripheral zone of 10 to 15 μm width free from microstructural damage.

The specimens preheated at 1000 and 1100°C prior to final heating at 1400°C displayed generally the same grain separations as specimens heated at 1400°C without pretreatment. Representative microstructures are shown in Figure 26. In particular, the observed width of the damage-free zones at the periphery of the high-density regions was about the same for the pretreated specimens as for the specimens heated directly to 1400°C. These observations indicated, as previously determined, that release of helium during preheating below damage thresholds was not sufficient to prevent microstructural damage during subsequent heating above threshold temperatures.

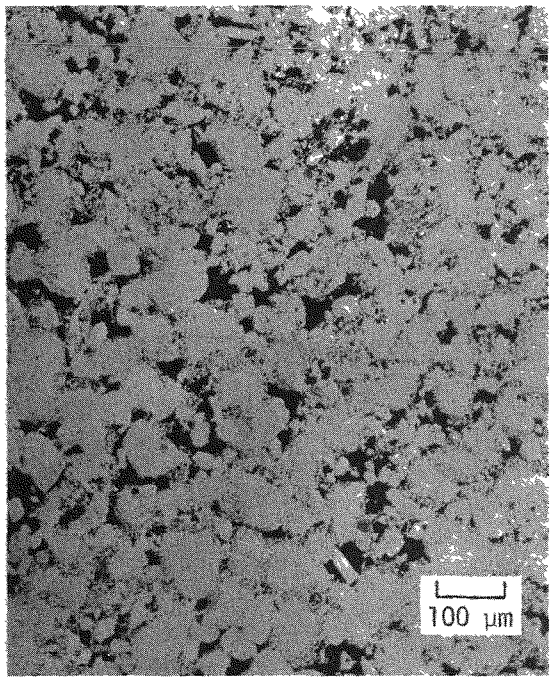

MHP 42-2A, Etched 1/2 hr

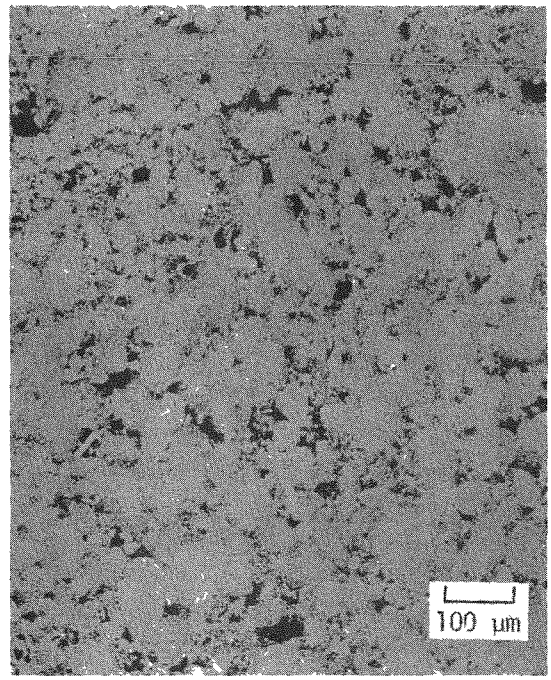

MHP 42-4A, Etched 1/2 hr

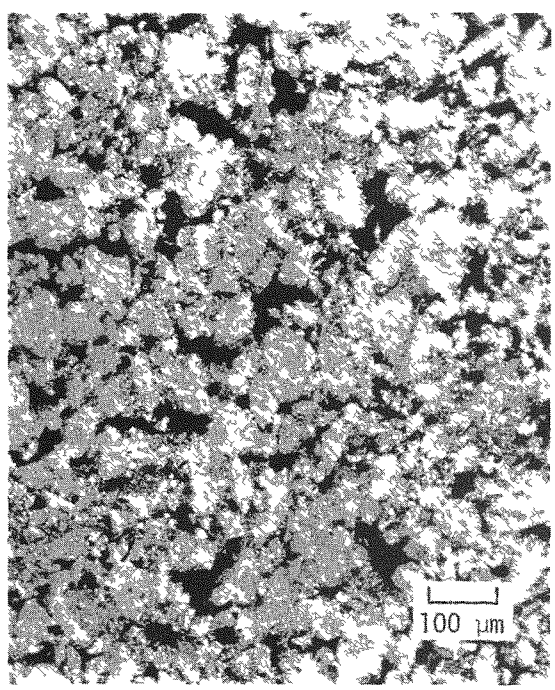

MHP 41-2A, Etched 2 hr

FIGURE 24. Typical Microstructures of 80% - Dense $^{238}PuO_2$ Pellets After Fabrication and 30-mo Aging. No differences from as-fabricated structures are apparent.

TABLE 6

Conditions for Heat Treatment of Aged $^{238}PuO_2$ Specimens

Specimen Number	*Temperature, °C*	*Time, hr*
MHP 42-2A	Not Heated	-
B	1400	3
C	1300	4
D	1500	3
MHP 42-4A	Not Heated	-
B	1200	4
C	1100	4
D	1000	4
MHP 41-2A	Not Heated	-
B	1000	3
	1400	1
C	1100	3
	1400	1
D	1400	1

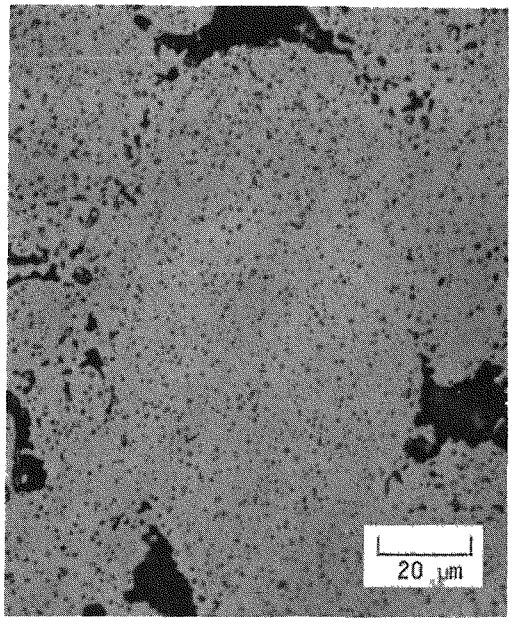

a. MHP 42-4A, Not Heated

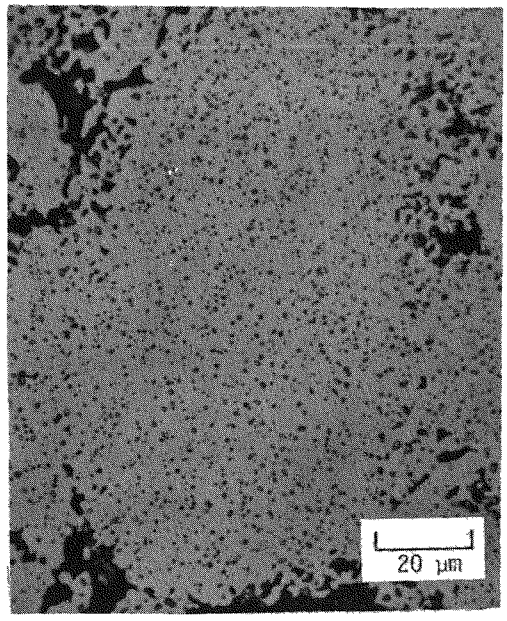

b. MHP 42-2A, Not Heated

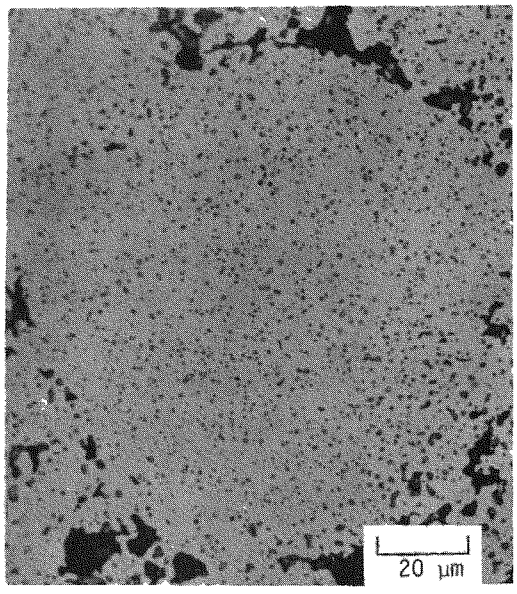

c. MHP 42-4D; Heated 1000°C, 4 hr

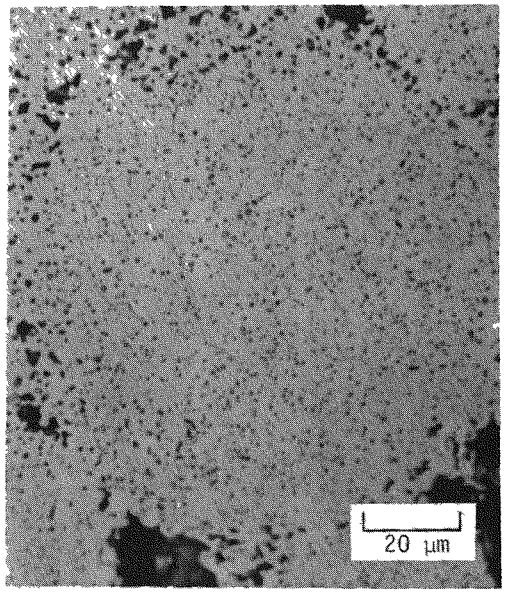

d. MHP 42-4C; Heated 1100°C, 4 hr

FIGURE 25. Microstructures of 30-mo Aged $^{238}PuO_2$ Pellet Segments Heated as Indicated. Etched 1/2 hr. Note well-defined grain separations caused by helium agglomeration in segments heated at 1200°C and higher.

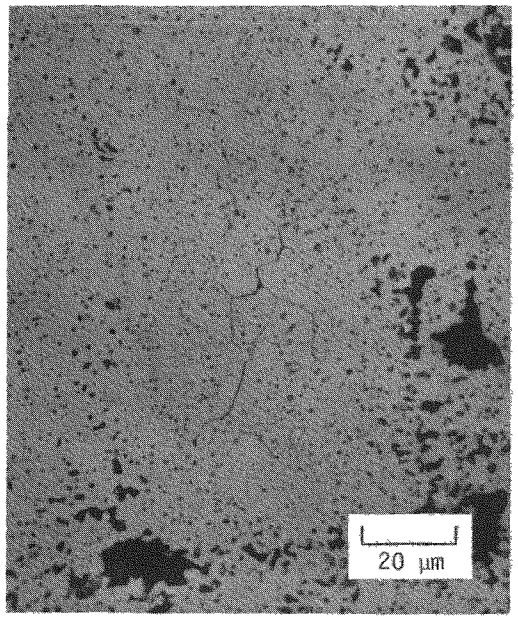

e. MHP 42-4B; Heated 1200°C, 4 hr

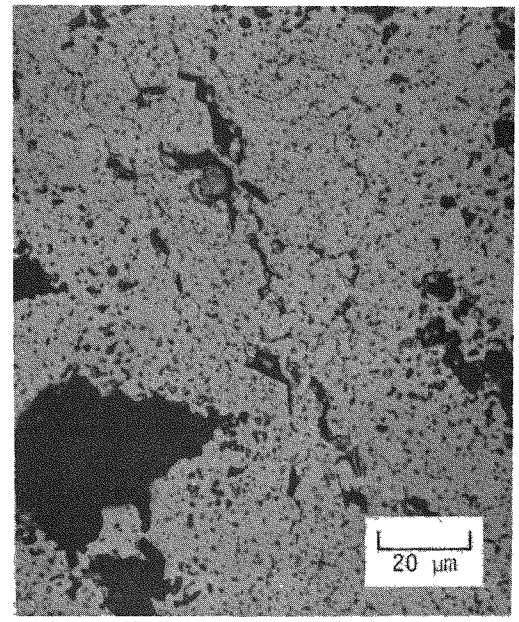

f. MHP 42-2C; Heated 1300°C, 4 hr

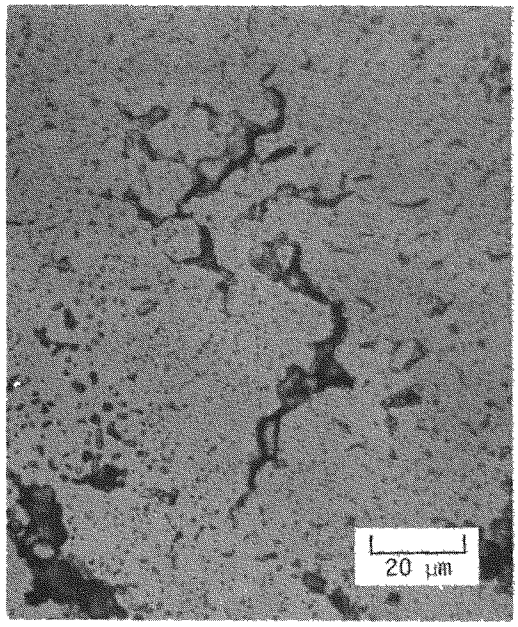

g. MHP 42-2B; Heated 1400°C, 3 hr

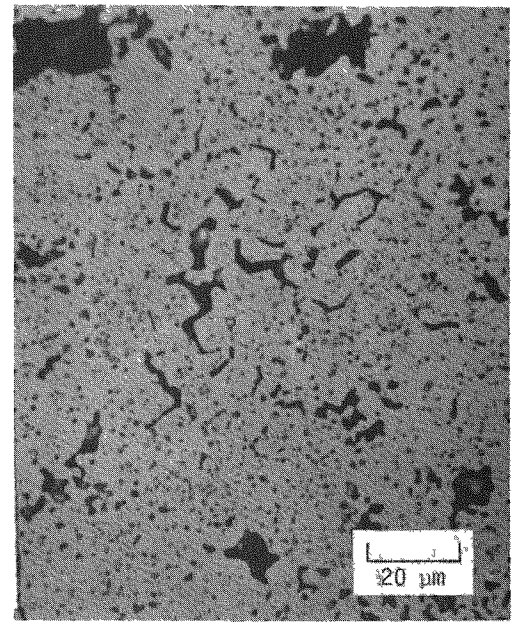

h. MHP 42-2D; Heated 1500°C, 3 hr

FIGURE 25, (Continued)

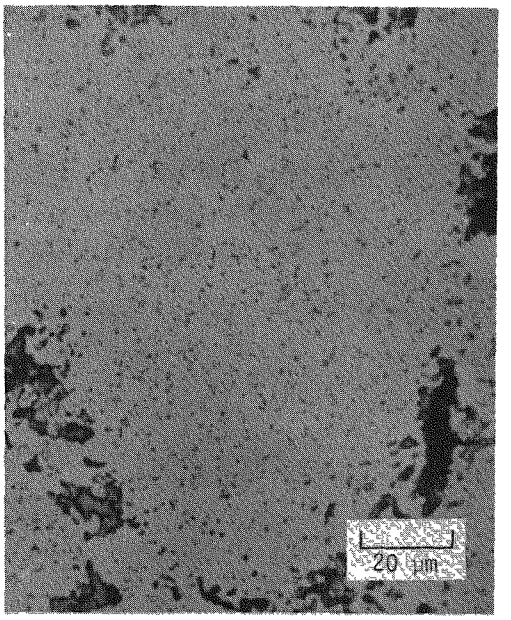

a. MHP 41-2A, Not Heated

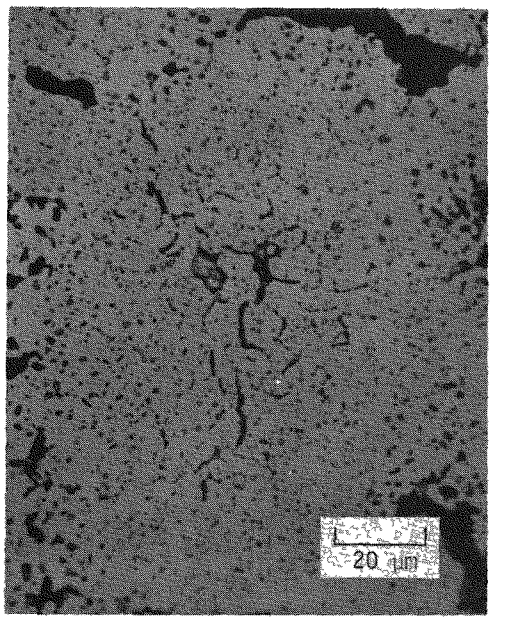

b. MHP 41-2B; Heated 1000°C, 3 hr and 1400°C, 1 hr

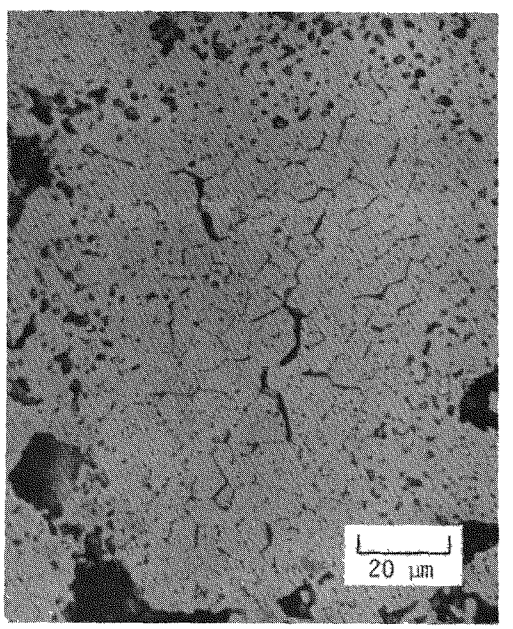

c. MHP 41-2D; Heated 1100°C, 3 hr and 1400°C, 1 hr

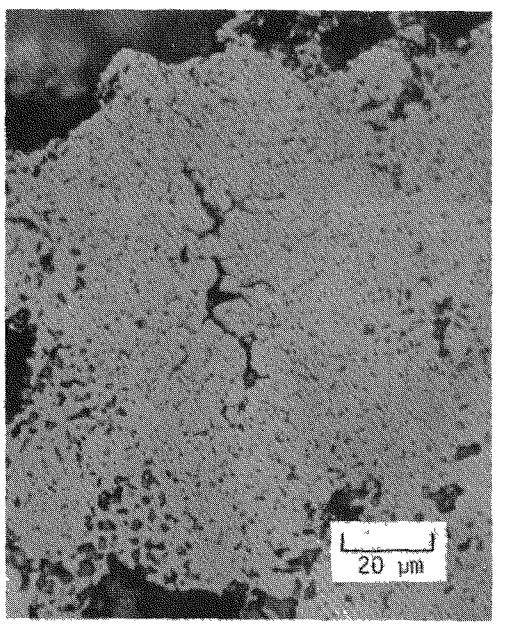

d. MHP 41-2D; Heated 1400°C, 1 hr

FIGURE 26. Microstructures of Aged $^{238}PuO_2$ Pellets Heated Following Pre-Heat Treatments as Indicated. Etched 1/2 hr. Note grain separations in all heated specimens.

Damage Mechanisms

Helium generated by alpha decay in $^{238}PuO_2$ specimens during aging agglomerates at high temperatures into bubbles at grain boundaries.[14,15] Eventual interconnection of these bubbles provides continuous channels for the primary release of the helium.[15,16] The microstructural damage observed in aged $^{238}PuO_2$ specimens after heating above 1200°C is presumably a remnant effect of this helium release process.

Previously, the edge-to-center decrease in severity of grain separations in the high-density areas of the small-grained pellets was believed to result from helium depletion by a second release mechanism, such as grain-boundary diffusion, below threshold temperatures for grain separation.[17] The tests described above, however, indicate that pretreatments at temperatures below damage threshold are not effective in preventing damage subsequently sustained above threshold temperatures, and thus, suggest that the damage-free peripheral zones do not result from a subthreshold helium depletion. The interior-to-edge gradation in severity of grain separations within the high-density regions of small-grained $^{238}PuO_2$ pellets must therefore be a result of the primary high-temperature release process.

Studies of fission gas transport and release in irradiated UO_2 fuels have shown that interlinking of grain-boundary bubbles on grain faces allows transfer of the accumulated gas to grain edges, where a dynamically stable configuration of interconnected tunnels is eventually formed.[18-20] Release of gas to the interconnected tunnels should allow the grain faces to resinter closed, until sufficient gas is again accumulated to form bubbles. In the small-grained $^{238}PuO_2$, however, separations at grain faces are apparently stabilized by the interconnected tunnels at grain edges and became part of the network of open channels which allow helium gas release. This network diminishes near the edges of the high-density regions as proximity to a free surface decreases the need for open channels to release accumulated helium.

Microstructural Specification of Damage-Resistant $^{238}PuO_2$ Forms

The observation of a damage-free zone at the edges of the high-density regions in small-grained $^{238}PuO_2$ pellet provides the basis for the following specification of a damage-resistant microstructure in $^{238}PuO_2$ heat source forms: the high-density regions in the microstructure should be no greater than about 25 μm in width, which is about equivalent to two thicknesses of the damage-free zone observed on structures with larger high-density regions. This specification applies principally to intermediate-density

(75 to 88% TD) forms, which have sufficient porosity for escape of the helium released from high-density regions. In this density range, the size of the high-density regions of a microstructure is limited by the size of the feed particles used in fabrication of the specimen.

Microstructural characteristics of $^{238}PuO_2$ forms produced by the direct fabrication process appear to meet this specification. In the direct fabrication process, $^{238}PuO_2$ feed particles prepared using reverse-strike precipitation of Pu^{4+} oxalate are directly hot-pressed into source forms ranging 75 to 90% TD (November 1976 report, p. 5[17]; April 1977 report, p. 7[21]). Average size of the feed particles varies from 8 to 20-μm yielding fabricated forms with equivalent size high-density regions. Effects of helium release treatments on the microstructure of directly fabricated $^{238}PuO_2$ specimens will be characterized in future tests.

EXPERIMENTAL FACILITIES

PLUTONIUM EXPERIMENTAL FACILITY (PEF)

Critical modifications and repairs to PEF have been completed so that Glove Boxes through Glove Box 9 can be closed up and simulant tests using ThO_2 started in early March. All major systems and equipment items have been functionally tested through Box 9. Glove Box 10 and beyond will not be used until the multipurpose welder planned for Glove Box 10 is installed (mid-FY 1979).

Installation of the replacement glove ports was completed. The new glove ports were leak tested, and the measured leak rate was significantly less than previously measured with the sphincter ports. Gaskets around windows and seams were retested for helium leak tightness. Functional tests of the two inert gas purification/recirculation systems indicated that impurity leakage rates of new glove ports improved by an order of magnitude.

The leak in the hot-press vacuum chamber was successfully repaired and helium-leaktested. The jacket was refilled with deionized water and will be flushed for about three weeks. After the jacket is flushed, the water will be drained and replaced with an inhibitor solution to retard any further corrosion. Final checkout and functional testing of the hotpress by the vendor was completed. The final test (before ThO_2 simulant pressings) consisted of hot pressing a sphere of cerium oxide. The hydraulic system was tested to the maximum design load of 100 KIP. The heat zone was tested up to 1850°C.

Calibration of the sintering furnace was completed, and the furnace operated essentially as designed. The length of the "hot zone" was about 1 in. shorter than desired; however, this can be corrected by a minor design change of the heating element or by using heat shields inside the muffle tube.

One additional major modification of the facility, installation of a transfer lock between Glove Boxes 5 and 6, was completed. The transfer lock between Boxes 10 and 11 was removed and reinstalled between Boxes 5 and 6 to enable isolation of the inert gas zones (separate recirculator/purifiers service Glove Boxes 3-5 and Glove Boxes 6-9). This modification will provide operational flexibility needed for the Milliwatt Program. Minor modifications to the facility to improve operability and safety, such as the addition of two sample bagout ports in the hoods, have been completed.

VISITS AND OFFSITE TRIPS

P. K. Smith, W. R. McDonell, and T. H. Gould, Jr. (SRL) attended a meeting at LASL on February 1 and 2 to discuss the need for future development work to improve current $^{238}PuO_2$ fuel forms.

REFERENCES

1. *Savannah River Laboratory Monthly Report, ^{238}Pu Fuel Form Processes, November/December 1977.* USDOE Report DPST-77-128-11/12, E. I. du Pont de Nemours & Company, Savannah River Laboratory, Aiken, SC (1978).

2. *Savannah River Laboratory Monthly Report, ^{238}Pu Fuel Form Processes, September 1977.* USERDA Report DPST-77-128-9, E. I. du Pont de Nemours & Company, Savannah River Laboratory, Aiken, SC (1977).

3. *Savannah River Laboratory Monthly Report, ^{238}Pu Fuel Form Processes, May 1977.* USERDA Report DPST-77-128-5, E. I. du Pont de Nemours & Company, Savannah River Laboratory, Aiken, SC (1977).

4. T. K. Keenan, R. A. Kent, and R. W. Zocher. *The Relationship of Fabrication Parameters to Selected Properties of $^{238}PuO_2$ Radioisotopic Fuels.* USERDA Report LA-5622-MS, Los Alamos Scientific Laboratory, Los Alamos, NM (1974).

5. *Savannah River Laboratory Monthly Report, ^{238}Pu Fuel Form Processes, October 1977.* USDOE Report DPST-77-128-10, E. I. du Pont de Nemours & Company, Savannah River Laboratory, Aiken, SC (1978).

6. *Savannah River Laboratory Monthly Report, ^{238}Pu Fuel Form Processes, July 1976.* USERDA Report DPST-76-128-7, E. I. du Pont de Nemours & Company, Savannah River Laboratory, Aiken, SC (1976).

7. *Savannah River Laboratory Monthly Report, ^{238}Pu Fuel Form Processes, May 1974.* USAEC Report DPST-74-128-5, E. I. du Pont de Nemours & Company, Savannah River Laboratory, Aiken, SC (1974).

8. *Savannah River Laboratory Monthly Report, ^{238}Pu Fuel Form Processes, July 1974.* USAEC Report DPST-74-128-7, E. I. du Pont de Nemours & Company, Savannah River Laboratory, Aiken, SC (1974).

9. J. J. Petrovic, S. S. Hecker, C. C. Land, and D. L. Rohr. *Mechanical Properties of $^{238}PuO_2$.* USERDA Report LA-6529, Los Alamos Scientific Laboratory, Los Alamos, NM (1977).

10. V. E. Hilliard. "Estimating Grain Size by the Intercept Method." *Met. Prog., 85,* 99 (1964).

11. *Savannah River Laboratory Monthly Report, ^{238}Pu Fuel Form Processes, August 1977.* USERDA Report DPST-77-128-8, E. I. du Pont de Nemours & Company, Savannah River Laboratory, Aiken, SC (1977).

12. *Savannah River Laboratory Monthly Report, ^{238}Pu Fuel Form Processes, April 1975.* USAEC Report DPST-75-128-4, E. I. du Pont de Nemours & Company, Savannah River Laboratory, Aiken, SC (1975).

13. *Savannah River Laboratory Monthly Report, ^{238}Pu Fuel Form Processes, July 1975.* USERDA Report DPST-75-128-7, E. I. du Pont de Nemours & Company, Savannah River Laboratory, Aiken, SC (1975).

14. B. A. Mueller, D. Douglas Rohr, and R. N. R. Mulford. *Helium Release and Microstructural Changes in $^{238}PuO_2$.* USAEC Report LA-5524, Los Alamos Scientific Laboratory, Los Alamos, NM (April 1974).

15. W. R. McDonell, J. E. Sheehan, and R. D. Sisson. "Helium Bubbles at Grain Boundaries of High-Density $^{238}PuO_2$ Shards." *ANS Trans. 22,* 214 (1975).

16. W. R. McDonell and D. T. Rankin. "Microstructural Damage Produced by Helium Release from $^{238}PuO_2$ Pellets." *Basic Sciences, Electronics and Nuclear Divisions Joint Fall Meeting, American Ceramic Society, San Francisco, CA, October 31-November 3, 1976, Ceramic Bull. 55,* 821 (1976).

17. *Savannah River Laboratory Monthly Report, ^{238}Pu Fuel Form Processes, November 1976.* USERDA Report DPST-76-128-11, E. I. du Pont de Nemours & Company, Savannah River Laboratory, Aiken, SC (1977).

18. W. Beere and G. L. Reynolds. "The Morphology and Growth Rate of Interlinked Porosity in Irradiated UO_2." *J. Nucl. Mater. 47,* 51 (1973).

19. J. A. Turnbull and M. O. Tucker. "Swelling in UO_2 Under Conditions of Gas Release." *Phil. Mag. 30,* 47 (1974).

20. C. C. Dollins and F. A. Nichols. "Swelling and Gas Release in UO_2 at Low and Intermediate Temperatures." *J. Nucl. Mater. 6,* 143 (1977).

21. *Savannah River Laboratory Monthly Report, ^{238}Pu Fuel Form Processes, April 1977.* USERDA Report DPST-77-128-4, E. I. du Pont de Nemours & Company, Savannah River Laboratory, Aiken, SC (1977).